Preprints.org

Article

Growth Developmental Defects of Mitochondrial Iron Transporter 1 and 2 Mutants in Arabidopsis in Iron Sufficient Conditions

Joaquin Vargas , Isabel Gómez , Elena Vidal , Chun Pong Lee , A. Harvey Millar , Xavier Jordana ,
Hannetz Roschzttardtz [*]

Article

Growth Developmental Defects of Mitochondrial Iron Transporter 1 and 2 Mutants in Arabidopsis in Iron Sufficient Conditions

Joaquín Vargas [1], Isabel Gómez [1], Elena Vidal [2,3,4], Chun Pong Lee [5], A. Harvey Millar [5], Xavier Jordana [1] and Hannetz Roschzttardtz [1]

[1] Departamento de Genética Molecular y Microbiología, Facultad de Ciencias Biológicas, Pontificia Universidad Católica de Chile, 8331150 Santiago, Chile.

[2] ANID-Millennium Science Initiative Program-Millennium Institute for Integrative Biology (iBio), 8331150 Santiago, Chile.

[3] Centro de Genómica y Bioinformática, Facultad de Ciencias, Ingeniería y Tecnología, Universidad Mayor, 8580745 Santiago, Chile

[4] Escuela de Biotecnología, Facultad de Ciencias, Ingeniería y Tecnología, Universidad Mayor, 8580745 Santiago, Chile

[5] ARC Centre of Excellence in Plant Energy Biology and School of Molecular Sciences, The University of Western Australia, Bayliss Building M316, Crawley, WA 6009, Australia.

* Correspondence: Prof. H. Roschzttardtz, Departamento de Genética Molecular y Microbiología, Facultad de Ciencias Biológicas, Pontificia Universidad Católica de Chile, Alameda Bernardo O'Higgins 340, 8331150 Santiago, Chile; Phone 56-223542669; e-mail: hroschzttardtz@bio.puc.cl

Abstract: Iron is the most abundant micronutrient in plant mitochondria and it has a crucial role in biochemical reactions involving electron transfer. It has been described in *Oryza sativa* that *Mitochondrial Iron Transporter* (*MIT*) is an essential gene and that knockdown mutant rice plants have a decreased amount of iron in mitochondria, strongly suggesting that OsMIT is involved in mitochondrial iron uptake. In *Arabidopsis thaliana*, two genes encode MIT homologues. In this study, we analyzed different *AtMIT1* and *AtMIT2* mutant alleles, confirming that individually *AtMIT1* nor *AtMIT2* genes are essential. When we generated crosses between *Atmit1* and *Atmit2* alleles we were able to isolate homozygous double mutant plants. Interestingly, homozygous double mutant plants were obtained only when mutant alleles of *Atmit2* with the T-DNA insertion in the intron region were used for crossings, and in these cases a correctly spliced *AtMIT2* mRNA was generated, although at a low level. *Atmit1 Atmit2* double homozygous mutant plants, which were knockout for *AtMIT1* and knockdown for *AtMIT2*, were grown and chacterised in iron sufficient conditions. Pleiotropic developmental defects were observed including abnormal seeds, increased number of cotyledons, slow growth rate, pinoid stems, defects in flower structures and reduced seed set. We observed a possible phenomenon of T-DNA suppression in the next generation of *Atmit1 Atmit2* double homozygous mutant plants, correlating with an increased splicing of the A*tMIT2* intron containing the T-DNA. Molecular analysis of gene expression markers for mitochondrial and oxidative stress showed that *Atmit1 Atmit2* double homozygous mutant plants express a degree of mitochondrial perturbation. A RNA-Seq study was performed and we could identify more than 760 genes differentially expressed in *Atmit1 Atmit2*, including genes involved in iron transport, coumarin metabolism, and hormones metabolism, transport and signaling. Our data suggest that some of the phenotypes observed in *Atmit1 Atmit2* double homozygous mutant plants are mediated by defects in auxin homeostasis.

Keywords: mitochondria; iron transporters; MIT; developmental defects; RNA-seq

1. Introduction

Iron is an essential nutrient and it is well-known that it is an integral constituent of many metalloproteins, primarily as part of heme groups and iron-sulfur clusters. As such, iron is essential for oxygen transport, electron transfer (redox) and catalytic reactions (Papanikolaou and Pantopoulos, 2005). The biological versatility of iron is based on its capacity to be coordinated by

proteins and to act as electron donor and acceptor. Thus, iron can readily convert between its two common oxidation states Fe^{2+} and Fe^{3+}, by the loss or gain of one electron. However, iron is also potentially toxic due to its redox reactivity. Indeed, free iron acts as a catalyst of oxidative stress via Fenton reactions, which yields hazardous radicals with the capacity to attack cellular macromolecules and cause tissue damage. Consequently, a tight control of iron homeostasis is imperative to satisfy metabolic needs for iron, and to prevent the accumulation of toxic iron concentrations. Iron homeostasis involves all the processes that regulate the balance between iron uptake, its intracellular storage and utilization (Collins and Anderson, 2012).

In soil Fe^{2+} undergoes spontaneous aerobic oxidation to Fe^{3+}, which is virtually insoluble at physiological pH. This makes acquisition of iron by cells and organisms challenging, despite its high abundance. The mechanism of iron uptake in the roots of *Arabidopsis thaliana* is now well-described and it involves an acidification reduction-transport mechanism (Curie et al., 2009). Under iron deficiency, ferric chelates are solubilized by local rhizosphere acidification caused by the release of protons by the ARABIDOPSIS PLASMA MEMBRANE H^+-ATPase2 (AHA2; Santi and Schmidt, 2009). Solubilized Fe^{3+} ions are then reduced to Fe^{2+} by the REDUCTASE FERRIC REDUCTION OXIDASE2 (FRO2) (Robinson et al., 1999) and, finally, transported into the cell by the IRON TRANSPORTER IRON REGULATED TRANSPORTER1 (IRT1; Eide et al., 1996; Vert et al., 2002). The mechanisms governing the distribution of iron to specific organs, cells and organelles are still very poorly understood.

In plants, in addition to its role in the mitochondrial electron transport chain, common to eukaryotes, iron is essential for chloroplast photosynthesis, as shown by chlorosis of plants grown under iron-deficient conditions (Guerinot and Yi, 1994; Yi and Guerinot, 1996; Briat et al., 2015). A total of twenty-two iron atoms are required per photosynthetic electron transport chain (Schmidt et al., 2020). Iron import into the chloroplast was proposed to be performed by the PERMEASE IN CHLOROPLAST1 (PIC1) localized in the inner envelope of this organelle (Duy et al., 2007). *PIC1* knockout mutations result in dwarf plants with altered iron homeostasis. Before being transported into the chloroplast, iron is thought to be first reduced by the FERRIC REDUCTASE7 (FRO7), also localized in the chloroplast envelope (Jeong et al., 2008). Indeed, chloroplasts isolated from *fro7* loss-of-function mutants have significantly reduced iron content and altered photosynthetic complexes (Jeong et al., 2008). Iron remobilization from leaves chloroplasts seems to be mediated by YSL4 and YSL6 (Divol et al., 2013). Recently, it has been suggested that FPN3 has a role in the iron export from Arabidopsis chloroplast and mitochondria (Kim et al., 2021).

In plant mitochondria, iron is more abundant than other transition metals such as Cu, Zn and Mn, consistent with its crucial role as component in electron transfer reactions (Tan et al., 2010). It has been suggested that iron is transported to the mitochondria through the outer membrane by Voltage Dependent Anion protein Channels (VDACs), and then to the mitochondrial matrix by the Mitochondrial Carrier Family (MCF) transporters. MCF gene family, with more than fifty members in *Arabidopsis thaliana*, encodes membrane proteins containing six transmembrane domains (Haferkamp and Schmitz-Esser, 2012). Mitochondrial Iron Transporter (MIT), a member of the MCF in *Oryza sativa*, was the first mitochondrial iron transporter identified in plants (Bashir et al., 2011). Complementation studies using OsMIT demonstrated that it is able to transport iron into yeast mitochondria and its function is essential in *Oryza sativa*. Knockdown plants for *OsMIT* showed a decrease of iron content in mitochondria and in the aconitase activity, an iron-sulfur protein (Bashir et al., 2011). In *Arabidopsis thaliana* it has been described that two genes encode MIT proteins (Jain et al., 2019). Fusions with fluorescent proteins demonstrated that AtMIT1 and AtMIT2 localized to mitochondria, and plants knockout for *MIT1* and knockdown for *MIT2* showed mitochondrial defects when plants were grown in iron deficiency conditions (Jain et al., 2019). Both mitochondrial iron deficiency or excess seems to provoke oxidative stress in a mammalian model (Walter et al., 2002). In plants, mitochondrial iron deficiency or excess also affects mitochondrial function (Vigani et al., 2009; Kim et al., 2021), indicating that plant mitochondria have a crucial role in cellular metal homeostasis (Vigani et al., 2019).

In this article, we characterize *Atmit1 Atmit2* double mutant plants (knockout for *MIT1* and knockdown for *MIT2*) grown in iron sufficient conditions. These plants showed pleiotropic developmental defects, some of which strikingly resemble those found in auxin transport and sensing mutants. Transcriptomic data revealed a misregulation of genes involved in iron acquisition, synthesis of coumarins, formation of the Casparian strip, suberization and root hair development. Furthermore, we demonstrate unambiguously, by crossing knockout mutants for MIT1 and MIT2, that MIT function is essential in Arabidopsis.

2. Results

Isolation of mutants in the two Arabidopsis genes encoding mitochondrial iron transporters (MIT)

In Arabidopsis two genes (At1g07030 and At2g30160) encode proteins with high similarity to the rice <u>M</u>itochondrial <u>I</u>ron <u>T</u>ransporter (MIT) (Bashir et al., 2011, Vigani et al., 2016) and have recently been characterised (Jain et al. 2019). The Arabidopsis MIT isoforms share 82% peptide sequence identity and similarity, including the putative mitochondrial targeting peptide. Both are 66-67 % identical (77-78 % similar) to the rice MIT protein (excluding the putative mitochondrial targeting peptides). To evaluate the potential role of the Arabidopsis proteins as mitochondrial iron transporters, At1g07030 (*MIT2*) and At2g30160 (*MIT1*) were used to transform the *MRS3-MRS4* knockout yeast ($\Delta mrs3\Delta mrs4$). *Saccharomyces cerevisiae* Mrs3 and Mrs4 are members of the MCF responsible for transporting Fe into mitochondria under low-Fe conditions, and the double knockout $\Delta mrs3\Delta mrs4$ mutant grows poorly when Fe availability is low (Foury and Roganti, 2002; Mühlenhoff et al., 2003). Each Arabidopsis MIT isoform was able to complement the growth defect of $\Delta mrs3\Delta mrs4$ yeast cells (Supplemental Figure S1), indicating that they can act as mitochondrial iron carriers. Our results are largely in agreement with previous observations by Jain et al. (2019), with the exception of the lack of evidence for a significant difference in the efficiency of complementation by MIT1 and MIT2 (Supplemental Figure S1).

To explore MIT1 and MIT2 function in Arabidopsis we identified two and three T-DNA insertion mutant lines for *MIT1* and *MIT2*, respectively (Figure 1A, Supplemental Figures S2 and S3). The T-DNA insertion is located in exon 1 for both *mit1* mutants, causing an interruption in gene expression 200 bp and 53 bp downstream of the start codon in *mit1-1* and *mit1-2* respectively. In *mit2-1* and *mit2-3* mutants, the T-DNA is located in the intron (419 and 500 bp downstream of the 5' splice site), while *mit2-2* contains an insertion in the first exon (239 bp downstream of the start codon). We analyzed the progeny of selfed heterozygous *mit1-1*, *mit1-2* and *mit2-1* plants and found that the progeny did not deviate significantly from 1:2:1 (wild type: heterozygous: homozygous). Furthermore, homozygous mutant plants for each of the *mit1* alleles and *mit2* alleles did not show any phenotypic alteration when compared to wild type plants (data not shown).

Next, RT-PCR analysis of *MIT1* and *MIT2* expression was carried out to ascertain homozygous mutant plants obtained for all five mutants (Figure 1B) were truly null mutants (Figure 1C). Results show clearly that *mit1-1*, *mit1-2* and *mit2-2* plants are knockout mutants, expressing only the non-mutated *MIT* gene. Unexpectedly, *mit2-1* and *mit2-3* expressed *MIT2*, in addition to *MIT1*, and thus are not knockout mutants. Characterization of the two T-DNA/*MIT2* junctions in *mit2-1* (Supplementary Figure S3) showed that no major deletions or chromosomal rearrangements occurred during the T-DNA insertion, which is 4080 bp long (with deletions of 303 bp in the right border and 102 bp in the left border), and thus this insertion converts a 913 nt intron into one of 4993 nt. Sequencing of the two *MIT2* RT-PCR products obtained from *mit2-1* RNA demonstrated that the intron is correctly spliced. Splicing of long introns is very unusual in plants but is not without precedent (e.g. Chang et al., 2017). However, *MIT2* transcript level as determined by RT-qPCR is significantly decreased (Supplementary Figure S6), confirming that both *mit2-1* and likely *mit2-3* are knockdown mutants.
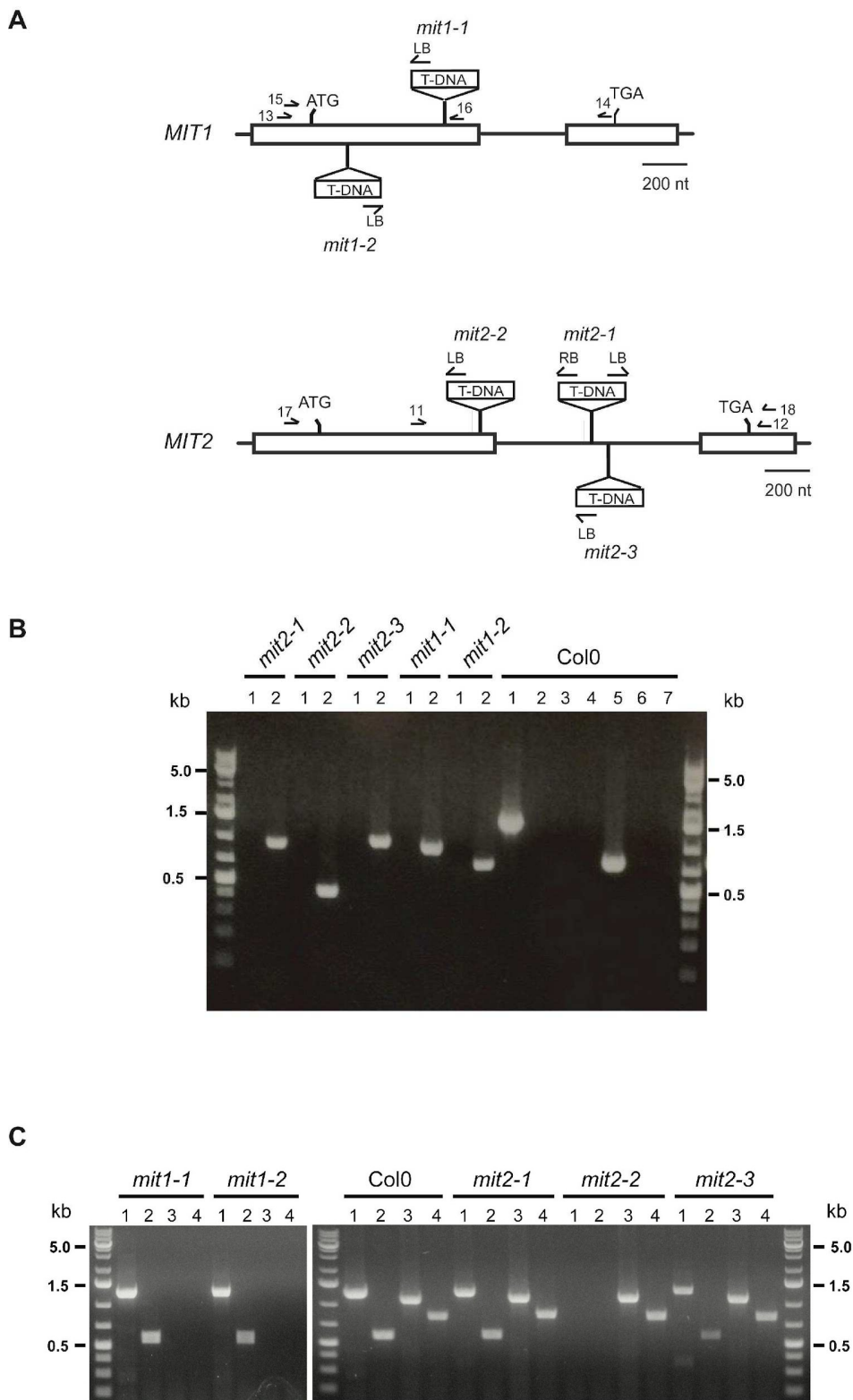
Figure 1. *Identification of mit1 and mit2 individual mutants*. **(A)** Exon-intron structure of *MIT* genes and T-DNA insertion sites. Exons are represented by boxes and T-DNA insertion sites in the different mutant lines are shown (T-DNA inserts are not drawn to scale) (details in Supplementary Figures S2 and S3). Horizontal arrows indicate the positions of primers. **(B)** Genotyping of individual *mit1* and *mit2* plants showing they are homozygous mutants. Lanes 1: PCR of the wild type allele (primers 11 and 12 for *MIT2*, 15 and 16 for *MIT1*); lanes 2: amplification of mutant alleles (primers LBb1.3 and 12 for *mit2-1*, 11 and LB1sail for *mit2-2*, 11 and LBb1.3 for *mit2-3*, 15 and LBb1.3 for *mit1-1*, LBb1.3 and 16 for *mit1-2*). PCR reactions with DNA from wild type Col0 plants were performed with all seven primer pairs (lanes 1 and 5: primers for wild type *MIT2* and *MIT1* alleles; lanes 2 to 4: primers for

mutant *mit2-1*, *mit2-2* and *mit2-3* alleles; lanes 6 and 7: primers for mutant *mit1-1* and *mit2-2* alleles). **(C)** *MIT2* and *MIT1* expression in individual *mit2* and *mit1* mutants. cDNAs from homozygous *mit2-1*, *mit2-2*, *mit2-3*, *mit1-1* and *mit1-2* mutant plants were amplified (40 cycles) with two primer pairs for each *MIT* transcript: 17 and 18 (lanes 1) or 11 and 12 (lanes 2) for *MIT2*, 13 and 14 (lanes 3) or 15 and 16 (lanes 4) for *MIT1*. Size standards correspond to the GeneRuler 1kb Plus DNA ladder from Thermo Scientific.

Given that *mit1-1*, *mit1-2* and *mit2-2* are knockout mutants their normal growth showed that neither *MIT1* nor *MIT2* are essential *per se*, and that they may be redundant. These results led us to perform *mit1* x *mit2* crosses.

2.1. MIT function is essential in Arabidopsis

Given that *mit1-1*, *mit1-2* and *mit2-2* are knockout mutants their normal growth showed that neither *MIT1* nor *MIT2* are essential *per se*. To determine whether MIT function is essential, we crossed the knockout mutants *mit1-1* and *mit2-2*. F2 seeds from selfed double heterozygous plants (*MIT1mit1-1 MIT2mit2-2*) were sown on 0.5X MS plates and a plant carrying three mutated alleles was identified (*MIT1mit1-1 mit2-2mit2-2*). Visual inspection of F3 seeds in three siliques from this selfed plant showed that they contain 77.5 ± 7.0 % normal seeds and 22.5 ± 7.0 % aborted seeds. Furthermore, when F3 seeds were allowed to developed on soil under iron-sufficient conditions, we were unable to identify a plant carrying a double homozygous mutation (65 plants analyzed). Altogether, these results confirm that MIT function is essential, that the absence of MIT1 and MIT2 is embryo-lethal, and that *MIT1* and *MIT2* genes are redundant.

2.2. Isolation of mit1-1 x mit2-1, a MIT knockdown mutant

Next, we crossed homozygous *mit1-1* with homozygous *mit2-1* plants. One hundred and seventy seven F2 plants grown from seeds of three selfed F1 double heterozygous plants (genotype *MIT1mit1 MIT2mit2*) were genotyped (Supplementary Table S2). No double homozygous mutants were identified, and we noted a bias against plants homozygous for *mit1* and heterozygous for *mit2* (4 plants *mit1-1mit1-1 MIT2mit2-1*) is apparent and not observed for plants heterozygous for *mit1* and homozygous for *mit2* (22 plants *mit1-1MIT1 mit2-1mit2-1*). This may be due to *mit1-1* being a knockout mutation and *mit2-1* a knockdown mutation (see below). The plants carrying three mutated alleles did not show visible phenotypic alterations when compared to wild type plants, at least under standard growth conditions.

Then F3 seeds from selfed F2 plants carrying three mutated alleles and one wild type allele (either *MIT1* or *MIT2*) were sown directly on soil and grown plants were genotyped. Again, no double homozygous mutant plants were obtained (73 and 65 plants analyzed, Table 1). These results suggest that MIT function is essential and that *MIT1* and *MIT2* genes are redundant. Furthermore, instead of the expected ratio of 2:1 for heterozygous: wild type plants, *MIT1mit1* : *MIT1MIT1* in the *mit2mit2* background, and *MIT2mit2* : *MIT2MIT2* in the *mit1mit1* background, ratios of 0.8 and 1.1 were observed. These ratios suggest a gametophytic defect, i.e. a defect in gametes carrying only mutated alleles of the mitochondrial iron transporters (*mit1mit2* gametes).

Table 1. Segregation analysis in the progeny of F2 plants carrying three mutated alleles.

Figure 2. plant genotype: *MIT1mit1mit2mit2*.

Analyzed F3 plants	Genotype of F3 plants		Ratio
	MIT1mit1mit2mit2	*MIT1MIT1mit2mit2*	
73	32	41	0.8

Figure 2. plant genotype: *mit1mit1MIT2mit2*.

Analyzed F3 plants	Genotype of F3 plants		Ratio
	mit1mit1MIT2mit2	*mit1mit1MIT2MIT2*	
65	34	31	1.1

F3 seeds obtained from selfed F2 plants carrying three mutated alleles were sown directly on soil and inheritance of *mit1* and *mit2* alleles were analyzed by genotyping 73 and 65 F3 plants, respectively. Uppercase letters indicate wild type alleles and lowercase letters mutated alleles. Seedling genotypes were determined by PCR as described in Methods. Expected ratio for Mendelian inheritance is 2.0.

Visual inspection of F4 seeds from F3 plants carrying three mutated alleles showed that in addition to "normal" seeds that resemble those from wild type plants, plants carrying three mutated alleles produced seeds with altered phenotypes: (i) smaller, irregular seeds ("abnormal" seeds), and (ii) shrunken, collapsed seeds ("aborted" seeds) (Figure 2A). Sets of normal, abnormal and aborted seeds per silique were quantitatively determined, using four *MIT1mit1 mit2mit2* plants, four *mit1mit1 MIT2mit2* plants and two wild type plants as control (Figure 2B). In siliques from plants with three mutated alleles, 26 % (plants with one *MIT1* wild type allele) and 20% (plants with one *MIT2* wild type allele) of total seeds were considered "abnormal". Only a minor proportion of seeds were aborted (7 % and 9 %, respectively). There are no significant differences in the total number of seeds per silique between wild type plants and plants with three mutated alleles, nor are significant numbers of non-fertilized ovules. Furthermore, these numbers were evenly distributed along the inflorescence axis, indicating that seed phenotypes are not due to flower heterogeneity (Supplementary Figure S4).
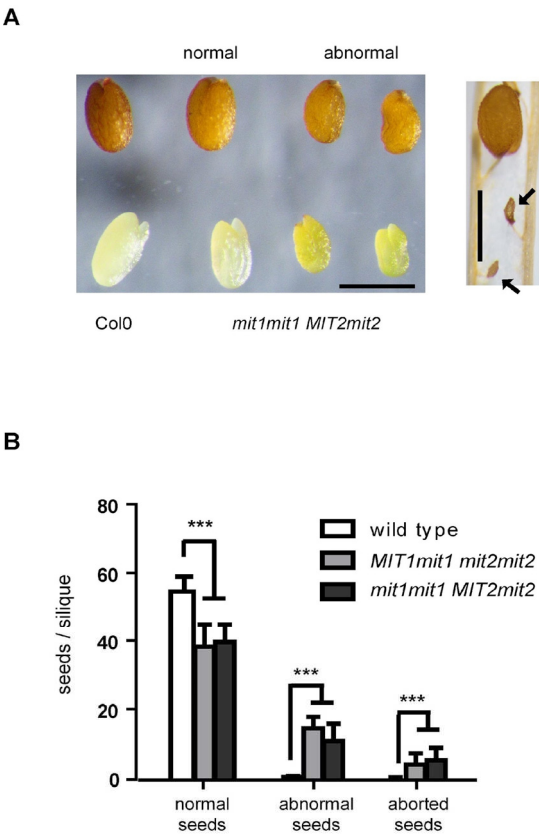
Figure 2. *Seed abnormalities in plants carrying three mit mutated alleles.* **(A)** Mature seeds and manually extracted embryos from wild type Col0 and *mit1mit1 MIT2mit2* plants. "Normal" seeds are those with a wild type phenotype, "abnormal" seeds and embryos are somewhat smaller and have an irregular surface. To the right is shown a silique fragment with two shrunken, collapsed seeds indicated by arrows. Bars = 500 μm. **(B)** Seed (normal, abnormal and aborted) set per silique was scored along the main inflorescence for four F3 *MIT1mit1 mit2mit2* plants, four F3 *mit1mit1MIT2mit2* plants and two wild type plants. Twelve siliques per plant (from the 5th to 16th in appearance) were scored. Error bars are SD. Asterisks indicate values that were determined by the *t*-test to be significantly different from wild type (***, p < 0.001).

When these "abnormal" seeds were sown on plates containing half-concentrated MS medium, almost all were able to germinate (Table 2) and expand their green cotyledons, although at a lower rate than "normal" and wild type seeds (Supplementary Figure S5). However, only around 50 % of seedlings were established with true leaves and elongated roots (Table 2). A significant proportion of these abnormal seeds possessed embryos with three cotyledons (Table 2, Figure 3). We were able to identify double homozygous mutants (*mit1-1mit1-1 mit2-1mit2-1*) among plants grown from "abnormal" seeds, in addition to plants with three mutated alleles (Figure 4). Furthermore, there is a strong correlation between growth rate and genotype: all double homozygous mutants presented a delayed growth rate when compared with plants with either 1 or 2 wild type *MIT1* alleles. These results showed on one hand that seed morphology was not a clear-cut criterion to identify genotype, and on the other hand that double homozygous mutants are viable. This unexpected result led us to determine that *mit2-1* is not a knockout mutant (see above, Figure 1C) and that *MIT2* is expressed, at a lower level (12.2%), in the double homozygous mutants (Supplementary Figure S6).

Table 2. Characterization of "abnormal" seeds obtained from plants with three mutated *mit* alleles.

	"Abnormal" seeds from	
	MIT1mit1mit2mit2	*mit1mit1MIT2mit2*
% germination	94.4 ± 7.8 [1]	97.2 ± 2.6 [2]
% establishment	57.4 [3]	53.9 ± 11.9 [4]
% 3-cotyledon embryos	12.1 ± 9.3 [5]	14.8 ± 8.4 [6]

Abnormal seeds of *MIT1mit1mit2mit2* and *mitmit1MIT2mit2* plants were sown on 0.5xMS plates and different parameters evaluated. Germination was recorded as radicle protrusion, establishment as appearance of leaves and root growth. [1] 5 replicates (20-30 seeds each), [2] 11 replicates (30-40 seeds each), [3] one experiment with 29 seeds, [4] 8 replicates (29-37 seeds each), [5] 5 replicates (15-33 seeds each, 15 embryos with 3 cotyledons out of 122 total abnormal seeds), [6] 10 replicates (30-40 seeds each, 48 3-cotyledon embryos out of 310 total abnormal seeds).

Five individual siliques from *MIT1mit1 mit2mit2* plants in two experiments were used to genotype all seedlings (established or not) grown from normal and abnormal seeds: 16.0 ± 3.5 % of total seeds were double homozygous mutants (43 out of 264 total seeds in the 5 siliques), and 27.7 ± 8.9 % of the double homozygous mutants possessed three cotyledons (11 plants out of 43). It is important to point out that all genotyped 3-cotyledon plants in this and other experiments were double homozygous mutants.
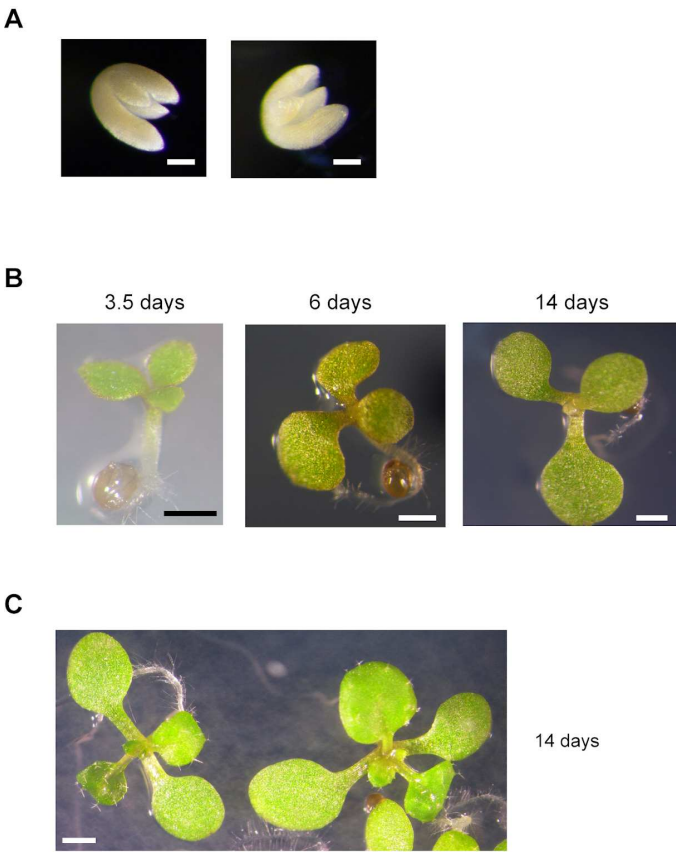
A

B

3.5 days   6 days   14 days

C

14 days

Figure 3. *Presence of three-cotyledon embryos in abnormal seeds.* **(A)** Manually extracted mature embryo (two views) from a *MIT1mit1 mit2mit2* plant. **(B)** Abnormal seeds from *mit1mit1 MIT2mit2* plants were sown on 0.5 x MS, stratified for 48 h and grown for 3.5, 6 and 14 days. The same plant bearing three cotyledons was photographed. (**C**) Control wild type plants grown for 14 days. Bars = 100 μm in **(A)**, 500 μm in **(B)**, 1000 μm in **(C)**.
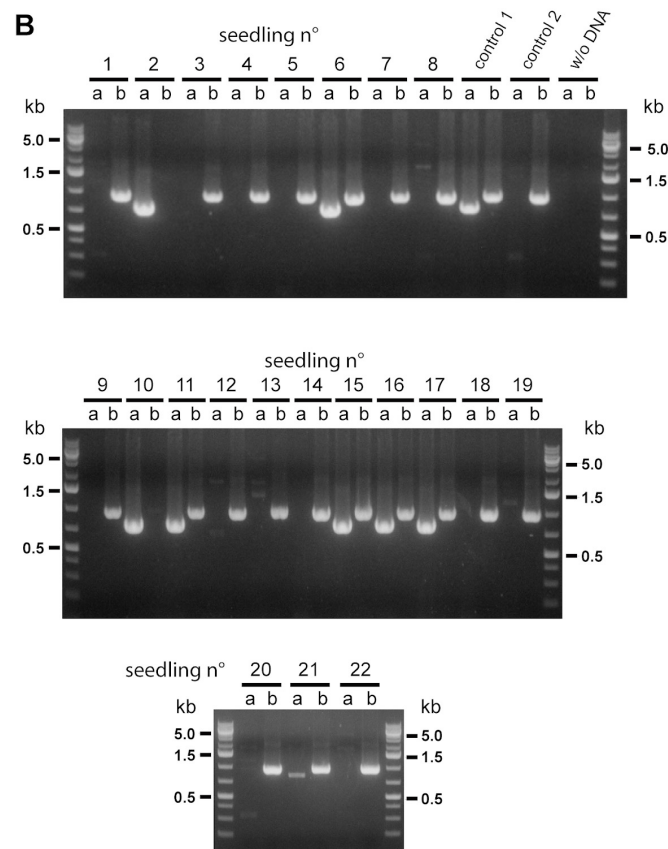
A

Figure 4. *Identification of double homozygous mutant plants.* **(A)** Twenty two abnormal seeds from a *MIT1mit1 mit2mit2* plant were grown on 0.5 x MS and genotyped **(B)** for the presence of the *MIT1* wild type allele (lanes a), using primers 15 and 16, and/or the *mit1-1* mutant allele (lanes b) using primers 15 and LBb1.3. Two plants have the *MIT1MIT1* genotype, 6 plants have the *MIT1mit1* genotype, and 14 plants have the *mit1mit1* genotype and are thus double homozygous mutant plants (*mit1mit1 mit2mit2*). Control 1 corresponds to DNA from a previously characterized double heterozygous plant (*MIT1mit1 MIT2mit2*) and control 2 to a homozygous *mit1-1mit1-1* plant.

2.3. Growth of double homozygous mutant plants is severely affected

Viable double homozygous *mit1-1mit1-1 mit2-1mit2-1* plants were easily identified by their severe phenotype. First, as already mentioned, germination and early post-germinative growth were slower than that of wild type plants and plants with three mutated alleles (Figure 4, Supplementary Figure S5). For instance, in one experiment, at 13 days when all Col0 seedlings (90 out of 90) were at least at stage 1.02 on day 13 according to Boyes et al. (2001), only one out of 59 (1.9%) of the double homozygous mutant seedlings attained this stage. Three weeks after germination, only 1.7 % (1/59) and 10 % (6/59) of these seedlings were at stages 1.06 and 1.04, respectively.

Growth of double homozygous mutant plants on soil was severely affected throughout the entire life cycle, and senescence was delayed by 1.5-2 months (Supplementary Figure S7). Drastic reduction of MIT expression has pleiotropic effects on double homozygous plants (Figure 5), including pinoid stems (Figure 5A and B) similar to those observed for mutants of auxin efflux carriers (PIN) (39 out of the 46 plants, 85 %), stems terminated at either cauline leaves (25 plants, 54%, Figure 5B), a unique flower (21 plants, 46%, Figure 5C) or multiple floral buds and cauline leaves (18 plants, 39%, Figure 5D). Furthermore, phyllotaxis in the appearance of cauline leaves was altered: there were a higher number of these leaves in some stems of 15 plants (33%, Figure 5E), their position was less regular (Figure 5D to F), and in some cases three cauline leaves were found at the same position (in 7 plants, 15%, Figure 5F). Additionally, some enlarged stems were found in 5 (11%) of the plants, as if two stems had been fused (Figure 5G, also visible in the plant shown in Figure 5F).
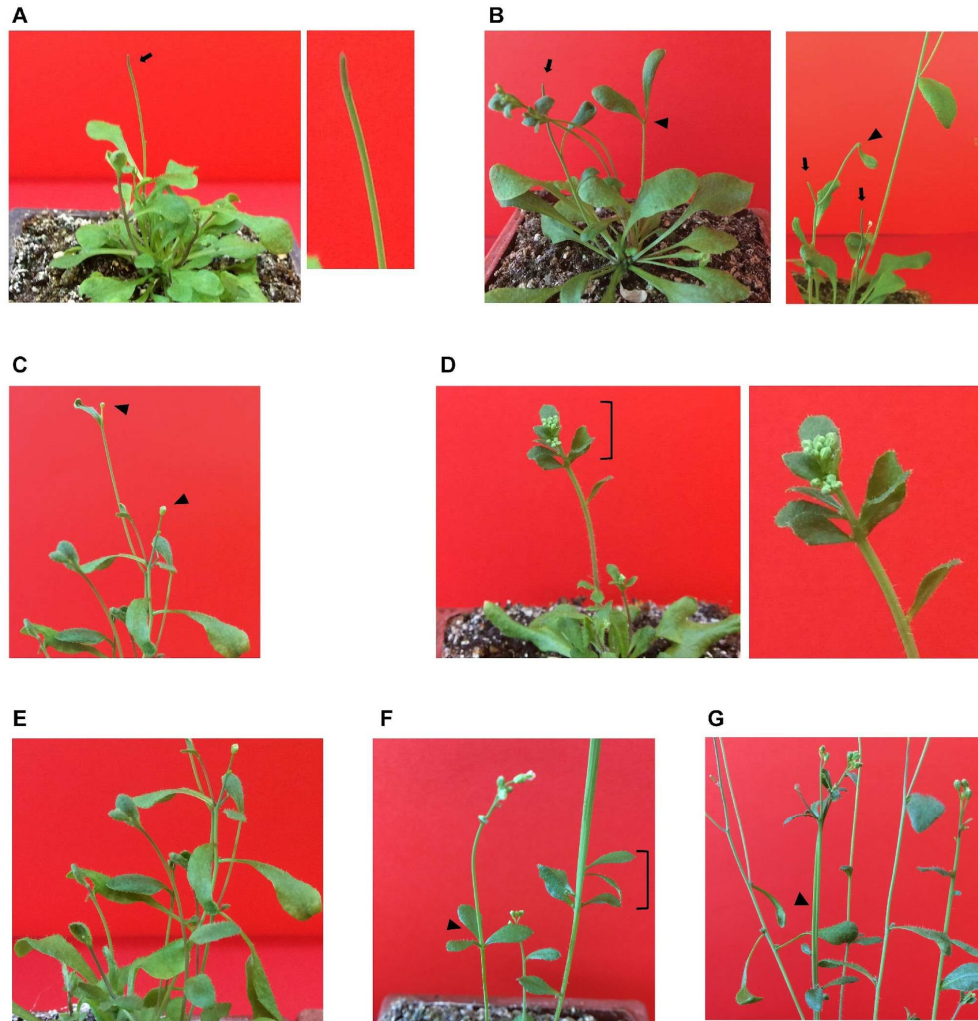
Figure 5. *Phenotypic alterations observed in double homozygous plants with drastic reduction of MIT expression.* **(A)** A pinoid stem (arrow) with the corresponding enlarged view. **(B)** Two plants with stems terminated at cauline leaves (arrowheads) and which also have pinoid stems (arrows). (**C**) A plant with stems terminated at unique flowers (arrowheads). **(D)** Multiple floral buds and cauline leaves at stem tip. **(E)** Higher number and irregular appearance of cauline leaves. **(F)** Three cauline leaves at the same position (arrowhead). **(G)** Enlarged stem (arrowhead).

All double mutant plants showed, alongside with some normal flowers, flowers with all their structures (sepals, petals, anthers, pistils) altered (Figure 6). This resulted in 17 out of 46 plants (37 %) unable to give seeds, and remaining plants showed a reduced seed set (less than 50 seeds in 1 to 6 siliques for 17 plants, between 50 and 250 seeds in 6 to 16 siliques for 10 plants, and more than 600 seeds for 2 plants with at least 80 siliques).
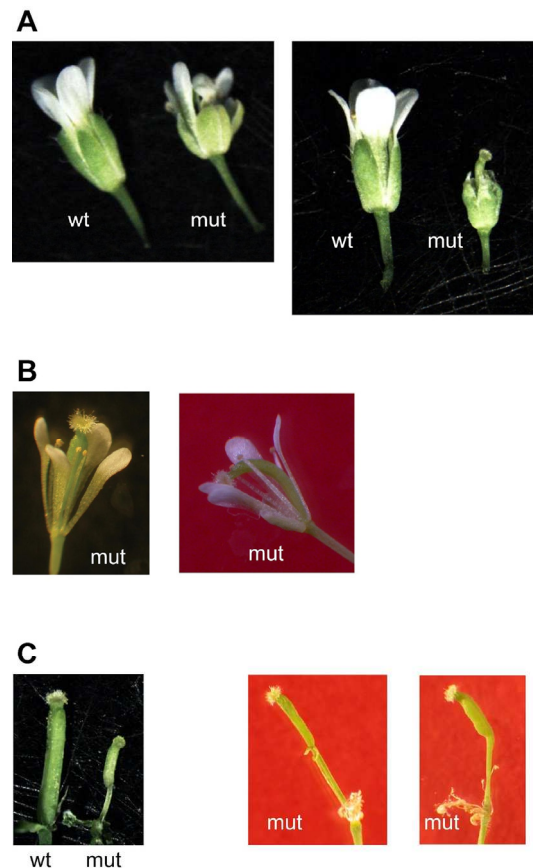
Figure 6. *Altered flowers in double homozygous plants with drastic reduction of MIT expression.* **(A)** Two different flowers from double homozygous *mit1-1 mit2-1* plants (mut) were compared with wild type (wt) flowers: smaller sepals, smaller petals, lack of anthers (right panel) were visible. **(B)** Two additional mutated flowers from which sepals have been excised: the four petals are heterogeneous in shape, abnormally positioned (right panel), only four and three anthers are present, pistil appears either normal (left panel) or curved (right panel). **(C)** Sepals, petals and anthers have been excised from wild type and mutated flowers: pistils with a stem-like base are frequent in mutated flowers.

2.4. The next generation of double homozygous mit1-1 mit2-1 mutant plants showed a normal phenotype

When seeds obtained from *mit1-1mit1-1 mit2-1mit2-1* plants were sown, almost all germinated (97.2 ± 5.0 %) and plant establishment was variable (55.5 ± 17.9 %). Most importantly, plant growth was similar to that of wild type plants, for instance all established seedlings were at stage 1.0 at 7 days and at stage 1.02-1.03 at 2 weeks, and this similarity extends to vegetative and reproductive growth. From now these plants have been designated as "compensated" double homozygous mutant plants. Their genotype was verified by PCR to be *mit1-1mit1-1 mit2-1mit2-1*.

This intriguing result led us to analyze *MIT2* expression by RT-qPCR in these "compensated" double homozygous mutant plants and compare it to that observed in plants showing an affected phenotype (first generation of double homozygous mutant plants, arising from seeds obtained from plants carrying three mutated alleles) (Figure 7). Interestingly, *MIT2* expression is significantly higher in compensated plants (60.9 % that of wild type plants) compared to affected plants (11.0 % - 18.5 % that of wild type).
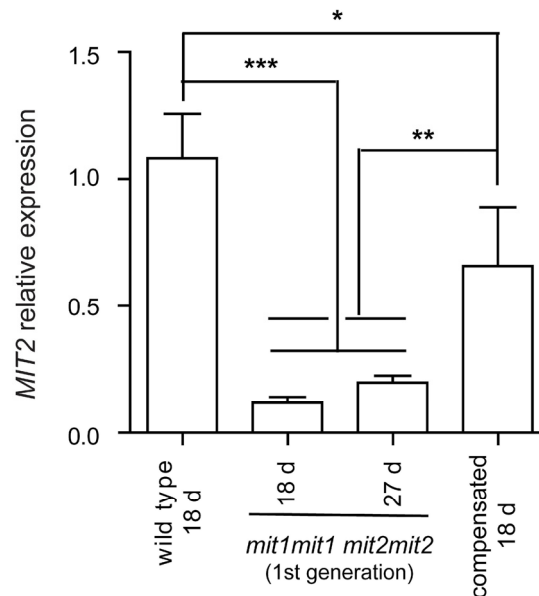
Figure 7. *MIT2 expression in double homozygous mutant plants*. MIT2 mature transcript levels were determined by RT-qPCR and normalized to *TIP41-like* transcript level. Means ± SD of four biological replicates are shown. RNAs were prepared from seedlings at stage 1.03-1.04 (Boyes et al., 2001), i.e. 18 days-old seedlings for wild type and "compensated" double homozygous mutant plants (*mit1-1mit1-1 mit2-1mit2-1*) and 27 days-old seedlings for the first generation of the double homozygous mutant plants (same developmental stage), and also from 18 days-old seedlings from these last plants (stage 1.0). The primers used for *MIT2* were primers 20 (encompassing exon junction) and 21 (Supplementary Table S1). Statistically significant differences were determined by one-way ANOVA followed by Tukey's multiple comparison test (***, $p < 0.001$; **, $p < 0.01$; *, $p < 0.05$).

These results are consistent with the view that increased splicing of the *MIT2* intron containing the T-DNA is responsible for phenotypic recovery of the double homozygous mutant plants, and may be related to a relatively recently described phenomenon called "T-DNA suppression" (see Discussion).

2.5. Analysis of mitochondrial function

Marker genes for mitochondrial response to stress have been identified (Van Aken et al., 2009), and included the genes encoding mitochondrial proteins alternative oxidase 1A and UPOX (up-regulated by oxidative stress) (Clifton et al., 2005; Ho et al., 2008). On the other hand, Van Aken and Whelan (2012) were able to identify marker genes that respond to mitochondrial and chloroplast dysfunction (e.g. *UPOX*) or are specific for mitochondrial dysfunction (e.g. *MSM1*, for Mitochondrial Stress Marker 1, also designated *At12cys-2*, Wang et al., 2016). We evaluated the expression of these three genes, *AOX1a*, *UPOX* and *MSM1*, and found that *UPOX* and *MSM1* are significantly up-regulated in the first generation of double homozygous mutant plants (*mit1-1mit1-1 mit2-1mit2-1*) but return to wild type levels in the "compensated" second generation plants (Figure 8). In contrast, *AOX1a* transcript levels were not significantly altered in any genotype. These results suggest some degree of mitochondrial perturbation in the first generation of double homozygous mutant plants with drastic reduction of *MIT* expression.
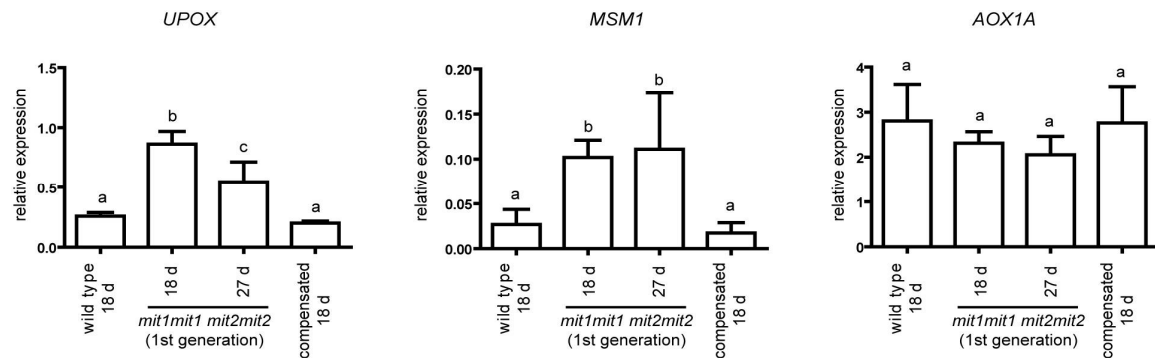
Figure 8. *Expression of UPOX, MSM1 and AOX1A in double homozygous mutant plants*. Transcript levels were determined by RT-qPCR and normalized to *TIP41-like* transcript level. Means ± SD of four biological replicates are shown. RNAs were prepared from seedlings at stage 1.03-1.04, i.e. 18 days-old seedlings for wild type and "compensated" double homozygous mutant plants (*mit1-1mit1-1 mit2-1mit2-1*) and 27 days-old seedlings for the first generation of the double homozygous mutant plants (same developmental stage), and also from 18 days-old seedlings from these last plants (stage 1.0). Primers sequences are indicated in Supplementary Table S1. Statistically significant differences were determined by one-way ANOVA followed by Tukey's multiple comparison test (same letter indicate no significant differences). For *UPOX*: a-b differences, $p < 0.001$; b-c differences, $p < 0.01$; for MSM1:   a-b differences, $p < 0.05$.

Unfortunately, we were unable to purify mitochondria from first generation double homozygous mutant plants (*mit1-1mit1-1 mit2-1mit2-1*) with an affected phenotype. To do this it would be necessary to grow plants with three mutated alleles, collect seeds, manually separate "abnormal" seeds and grow plants from these seeds; so it was unfeasible to obtain enough biological material. Thus, mitochondria were purified from "compensated" double homozygous mutant (*mit1-1mit1-1 mit2-1mit2-1*) and wild type seedlings as described in Supplementary Methods.

Targetted proteomic analysis was performed on 4 biological replicates of both compensated and wild-type mitochondria by Selective Reaction Monitoring (SRM) mass spectrometry. In this way more than one hundred proteins (listed in Supplementary Table S3) were quantified allowing a focused dissection of responses in the TCA cylce, electron transport chain, mitochondrial localised iron-related proteins, and MIT1/2 proteins (Supplementary Figure S8 A). Significant differences in protein levels between compensated and wild type plants were found only for MIT1 and MIT2. The specific quantified peptide for MIT1 was found in wild-type, but was below the limit of detection in mitochondria from "compensated" double homozygous plants (as expected for a knockout mutation). The specific peptide for MIT2 in compensated plants was 30.9 ± 12.4 (SD) % the level found in wild type mitochondria, confirming that *mit2-1* is a knockdown allele.

Despite this large reduction in MIT abundance (absence of MIT1, and 30 % of MIT2), no differences were observed in the oxygen consumption rate of isolated mitochondria (Supplementary Figure S8 B). Furthermore, no differences were detected in the abundance or native size of respiratory complexes or in complex I activity when analyzed by BN gel electrophoresis (Supplementary Figure S8C). Complex I activity was assessed as it is the respiratory complex having the higher number of iron ions in its structure present as iron-sulfur centers. These results show that, at least when plants are grown under standard conditions, mitochondria with a drastic reduction in MIT are not functionally impaired.

2.6. RNA-seq analysis of gene expression in double homozygous mutant plants

Since RNA-seq analysis required less biological material, we were able to perform this analysis with the first generation of double homozygous mutant plants (*mit1-1mit1-1 mit2-1mit2-1*) which showed an affected phenotype, and compare this transcriptome to that of "compensated" plants having the same genotype, and that of wild type plants. Total RNA was prepared from three

biological replicates of 18 days-old wild type seedlings and compensated double homozygous mutant seedlings. For double homozygous plants of the first generation (thus, presenting a severe phenotype), 27 days-old seedlings were considered in order to compare plants at the same developmental stage, in this case 1.04 of Boyes et al. (2001). Poly A-enriched RNA fractions were employed to construct libraries for Illumina sequencing (see Methods).

Differentially expressed genes between genotypes were identified ($padj < 0.05$, $\log_2$ [fold change] > 1 in any condition, LRT test) and grouped in two clusters by k-means (Figure 9). Interestingly, no significant differences (except for *MIT* expression) were found between wild type plants and compensated plants (Wald test, $padj = 3.08E-18$, $\log_2$ fold change = -4.2), further supporting the conclusion that partial expression (around 30 %) of one of the two *MIT* genes is sufficient for normal plant growth and development. In cluster 1 (408 genes, listed in Supplementary Table S4) expression is down regulated in double homozygous mutant plants (1st generation) when compared to wild type and compensated plants. In cluster 2 (360 genes, listed in Supplementary Table S5) higher levels of transcripts are found in the double homozygous mutant plants (1st generation).

A

B
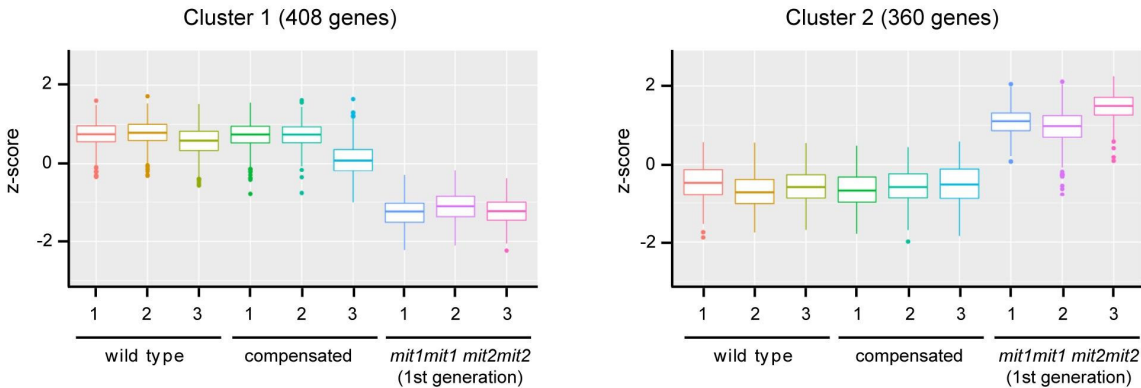
GO biological process	Fold Enrichment	FDR
cell-cell junction assembly (GO:0007043)	45.72	8.52E-04
coumarin metabolic process (GO:0009804)	38.10	1.38E-04
suberin biosynthetic process (GO:0010345)	24.94	1.27E-06
zinc ion transmembrane transport (GO:0071577)	14.91	3.94E-03
iron ion transport (GO:0006826)	14.69	8.55E-04
root hair elongation (GO:0048767)	7.12	2.82E-03
root hair cell differentiation (GO:0048765)	8.15	4.24E-08
trichoblast differentiation (GO:0010054)	9.08	2.65E-10
root epidermal cell differentiation (GO:0010053)	8.77	4.32E-11
root morphogenesis (GO:0010015)	5.85	6.10E-23
root system development (GO:0022622)	5.20	5.34E-34
plant-type cell wall modification (GO:0009827)	6.33	3.43E-02
cell wall organization or biogenesis (GO:0071554)	3.32	6.98E-10
unidimensional cell growth (GO:0009826)	3.04	9.83E-03

| GO biological process	Fold Enrichment	FDR
production of siRNA involved in gene silencing by small RNA (GO:0070919)	24.35	4.37E-02
heterochromatin assembly (GO:0031507)	7.85	2.31E-02
regulation of jasmonic acid mediated signaling pathway (GO:2000022)	20.29	3.59E-08
jasmonic acid metabolic process (GO:0009694)	13.25	1.35E-04
plant organ formation (GO:1905393)	5.07	3.19E-02
anatomical structure formation involved in morphogenesis (GO:0048646)	4.12	5.04E-03
response to jasmonic acid (GO:0009753)	4.70	5.99E-11
flower development (GO:0009908)	3.46	4.42E-04
response to wounding (GO:0009611)	4.17	1.99E-11
glucosinolate metabolic process (GO:0019760)	3.95	2.26E-02
floral organ development (GO:0048437)	3.69	2.23E-02
response to water deprivation (GO:0009414)	2.95	4.28E-06
response to other organism (GO:0051707)	1.81	3.27E-03
defense response (GO:0006952)	1.68	3.28E-02

Figure 9. *K-means clustering of differentially expressed genes.* RNAs were prepared from seedlings at the same developmental stage: wild type plants (18 days-old), compensated double homozygous mutant plants (18 days-old) and 1st generation of double homozygous mutant plants with an affected phenotype (27 days-old). RNAseq was performed on three biological replicates (seedlings grown in different days) for each group, differentially expressed genes (at least two-fold) were identified using DEseq2 software and clustered by k-means. **(B)** Some enriched GO terms (biological processes) in clusters 1 and 2. See Supplementary Tables S6 and S7 for more detailed information.

Enrichment of GO terms (biological processes) was analyzed in both clusters (Supplementary Tables S6 and S7).

Cluster 1 shows an overrepresentation of genes belonging to the Gene Ontology annotation categories of iron ion transport (GO:0006826; FDR 8.6×10^{-4}, 14.7 fold enrichment) and coumarin metabolic process (GO: 0009804; FDR 1.4×10^{-4}, 38.1 fold enrichment); coumarins being involved in iron chelation in the rhizosphere for incorporation into the plant (Rajniak et al., 2018; Tsai et al., 2018; Riaz and Guerinot, 2021). For instance, *FRO2* (At1g01580, ferric reduction oxidase 2), *IRT1* (At4g19690, iron-regulated transporter 1), *IRT2* (At4g19680, iron-regulated transporter 2), *FIT1/FRU/bHLH29* (At2g28160, FER-like Iron deficiency Induced-Transcription factor), *IREG2/FPN2*

(At5g03570, iron-regulated transporter 2, ferroportin 2), *BTSL2* (At1g74770, Zinc finger BRUTUS-like protein 2) and *NAS2* (At5g56080, nicotianamine synthase 2) are in cluster 1. Down regulation of *FRO2* and *IRT1* were also independently verified by RT-qPCR (Figure 10). Other relevant overrepresented biological processes in Cluster 1 are related to growth processes, including root hair elongation, plant-type cell wall modification and unidimensional cell growth, consistent with the growth deficiency phenotypes presented in the double homozygous mutants (Supplementary Table S6).
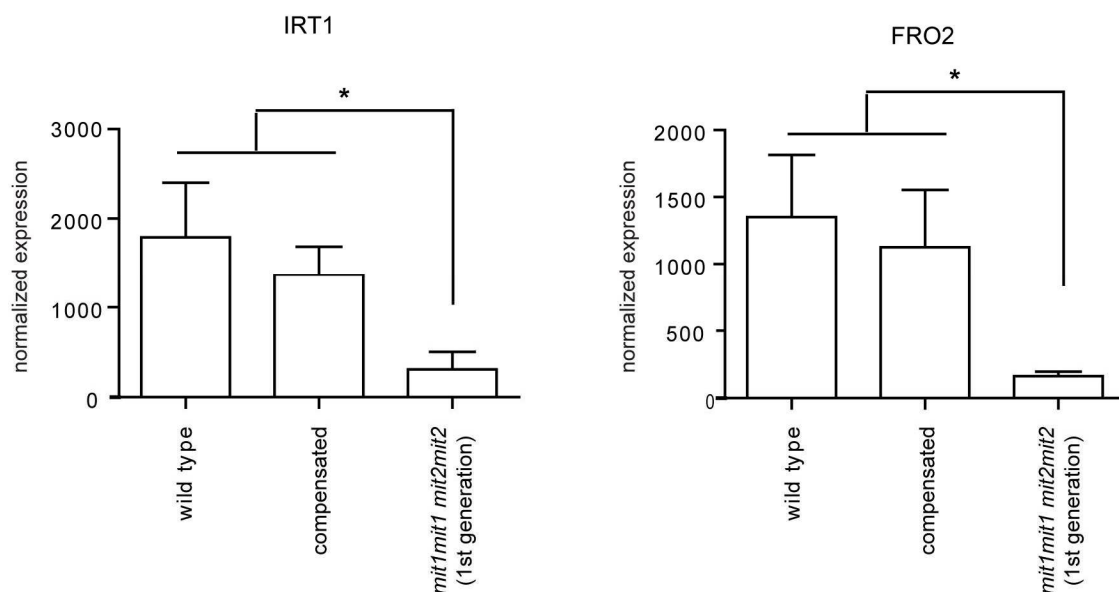
A RT-qPCR
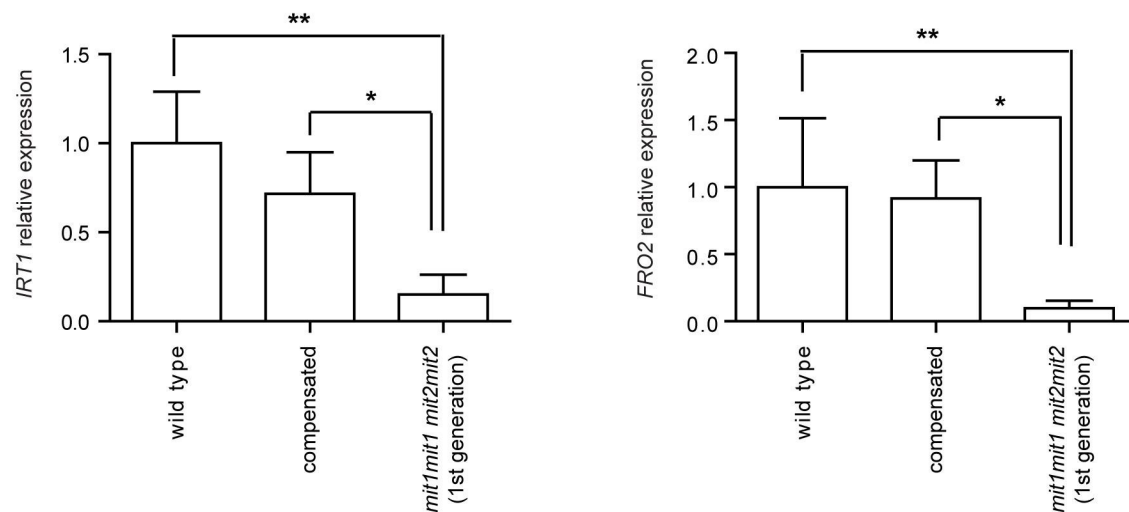
B RNAseq

Figure 10. *IRT1* and *FRO2 expression in double homozygous mutant plants*. (**A)** *IRT1* and *FRO2* mature transcript levels were determined by RT-qPCR and normalized to *TIP41-like* transcript level. RNAs were prepared from seedlings at stage 1.03-1.04 (same developmental stage). Primers sequences are indicated in Supplementary Table S1. Means ± SD of three (*IRT1*) or four (*FRO2*) biological replicates are shown. Statistically significant differences were determined by one-way ANOVA followed by Tukey's multiple comparison test (**, $p < 0.01$; *, $p < 0.05$). (**B**) Normalized expression of *IRT1* and *FRO2* as determined by RNAseq. Means ± SD of the three biological replicates are shown, a one-way ANOVA was performed, followed by Tukey's multiple comparison test (*, $p < 0.05$)...

Cluster 2, containing genes with an increased expression relative to wild-type and compensated plants, shows an overrepresentation of biological processes that can be related to plant defense, including different terms related to jasmonic acid (regulation of jasmonic acid mediated signaling pathway, jasmonic acid metabolic process, response to jasmonic acid), regulation of defense response, response to other organism and glucosinolate metabolic process. As well, processes related to wounding and response to water deprivation were found in cluster 2. This suggests that double homozygous plants have a basal activation of stress-related responses, which might impact plant growth in these plants.

3. Discussion

Arabidopsis *MIT1* and *MIT2* encode proteins highly similar to rice MIT and with significant similarity to yeast mitochondrial iron transporters MRS3 and MRS4 (38 % identity). Mitochondrial localization of the plant proteins has been demonstrated by either fusion to GFP or YFP (Bashir et al., 2011; Jain et al., 2019), subcellular fractionation (Jain et al., 2019), or proteomic analysis of purified mitochondria (Supplemental Figure 8). Expression of plant *MIT* genes appears to be ubiquitous (Bashir et al., 2011; Jain et al., 2019; http://bar.utoronto.ca). MIT1 and MIT2, with their own targeting peptides (Supplementary Figure S1) or that of MRS3 (Jain et al., 2019) were able to complement the defect of the yeast Δ*mrs3*Δ*mrs4* mutant, demonstrating that they function as high affinity iron transporters in yeast mitochondria, and likely also in plant mitochondria.

The rice *MIT1* gene is essential since its absence is embryo-lethal (Bashir et al., 2011). In contrast, in Arabidopsis *MIT1* and *MIT2* appear to be redundant since individual mutants, including the knockout mutants *mit1-1* and *mit2-2* were indistinguishable from wild type plants. However, MIT function is essential in Arabidopsis since when crossing these two null mutants no double homozygous plants could be obtained, and almost 25 % of the seeds from plants with three mutated alleles (*MIT1mit1-1 mit2-2mit2-2*) aborted.

3.1. Phenotypic alterations of the mit1-1 mit2-1 double homozygous mutants

When crossing the knockout *mit1-1* mutant with the knockdown *mit2-1* mutant we were able to obtain double homozygous mutant plants from the so-called "abnormal" seeds plated on MS x 0.5 (Figures 2 and 4). The 1st generation of these plants expressed only low levels of *MIT2* (10-20 %, Figure 7 and Supplementary Figure S6) and showed striking phenotypes, highlighting the importance of MIT function. Pleiotropic defects include polycotyly (three cotyledon-embryos, Figure 3 and Table 2), retarded germination and early post-germinative growth with reduced establishment (Supplementary Figure S5, Figure 4, Table 2), delayed and altered reproductive development including *pin* stems, abnormalities in phyllotaxy and in all organs of the flowers (Figures 5 and 6), and reduced seed set.

Some of these phenotypes are clearly indicative of defects in auxin signaling. For instance, it is well known that polar auxin transport is involved in cotyledon emergence (Liu et al., 1993; Benková et al., 2003), and both *pin* and *pid* mutants show polycotyly (Bennett et al., 1995; Benjamins et al., 2001; Aida et al., 2002; Furutani et al., 2004). However, whereas the presence of one cotyledon is more frequent in *pin1* mutants (auxin efflux carrier, PINFORMED1), mutants in the ser/thr protein kinase PID (PINOID) which phosphorylates PIN1, show higher frequency of three-cotyledon embryos, and thus resembles double homozygous *mit1-1 mit2-1* embryos. In all these cases phenotype penetrance is incomplete. Furthermore, striking similarities are found between *pin*, *pid* and *mit1-1mit2-1* mutants during reproductive development: inflorescence stems without flowers and cauline leaves (*pin* stems), alterations in cauline leaves phyllotaxis, abnormal flowers, reduced fertility (Figures 5 and 6; Okada et al., 1991; Bennett et al., 1995; Christensen et al., 2000).

Although somewhat surprising at first sight, an interplay between mitochondrial function and auxin signaling is well documented. For instance, an antagonistic relationship has been described between mitochondrial stress signaling (MRR, mitochondrial retrograde regulation) and auxin signaling (Kerchev et al., 2014; Ivanova et al., 2014). Furthermore, a knockdown mutant in a mitochondrial Pyruvate dehydrogenase subunit (*mab1-1*, *macchi-bou1*), which has reduced respiration

and pyruvate dehydrogenase activity, is also defective in polar auxin transport and shows auxin-related phenotypes (Ohbayashi et al., 2019). Knockdown of the succinate dehydrogenase assembly factor SDHAF2 is also known to induce ROS-mediated auxin hypersensitivity, causing pH-dependent root elongation   in Arabidopsis (Tivendale et al 2021). The exact mechanisms linking in each case mitochondrial dysfunction and auxin signaling are not known but several competing or complementary hypotheses have been proposed based on the deep connections between auxin synthesis, conjugation and post-translational regulation of auxin signalling pathways   (Tivendale and Millar 2022). These assembled examples and our results suggest that at least some of the phenotypes observed in the *mit1-1mit2-1* double homozygous mutants are mediated by defects in auxin homeostasis.

On the other hand, phenotypes like reduced plant establishment, delayed germination and slow early post-germinative growth are characteristic of mitochondrial deficiency. Seed germination and early post-germinative growth are crucial for seedling establishment and involved the mobilization of seed nutrient reserves to fuel growth until the seedling becomes photoautotrophic. Mitochondria are expected to play a crucial role at these early stages, supplying energy and carbon skeletons for growth, and a role for respiratory complexes I, II and IV has been described (e.g. de Longevialle et al., 2007; Meyer et al., 2009; Roschzttardtz et al., 2009; Kühn et al., 2015; Restovic et al., 2017; Kolli et al., 2019). For instance, Kühn et al. (2015) found a correlation between the severity of complex I mutants and the delay in germination, cotyledon emergence, and seedling establishment. Unfortunately, as already mentioned, we were unable to obtain mitochondria from these seedlings to assess mitochondrial function, and only indirect evidence for mitochondrial dysfunction, i.e. higher transcript levels of *MSM1* and *UPOX*, was documented (Figure 8). However, Bashir et al. (2011) characterized a knockdown mutant of the unique rice *MIT* gene (*mit-2*, T-DNA insertion in the gene promoter) which displays a less severe phenotype, allowing mitochondrial preparation from homozygous mutant plants. Those rice mitochondria contain less Fe and have less aconitase (an iron-sulfur protein) activity, thus supporting a mitochondrial dysfunction due to iron deficiency also in our Arabidopsis double mutant.

3.2. Phenotypic recovery of double homozygous mit1-1 mit2-1 in next generations

When the few seeds obtained from the affected *mit1-1mit1-1 mit2-1mit2-1* plants were sown, plant growth was similar to that of wild type plants. In these "compensated" double homozygous mutant plants, *MIT2* expression is enhanced with respect to parent plants (Figure 7), and   targeted proteomic analysis of purified mitochondria showed they differ significantly from wild type mitochondria only in MIT1 (undetectable) and MIT2 (30 %) content (Supplementary Figure S8). Furthermore, no differences were observed in mitochondrial respiratory rate, respiratory complex size and abundance or complex I activity. Thus, increased splicing of the *MIT2* intron containing the T-DNA is likely responsible for phenotypic recovery of the double homozygous mutant plants. In the past years a phenomenon called "T-DNA suppression" has been described, occurring when crossing two mutants with similar T-DNA insertions (e.g. two SALK lines). At least one of the T-DNA insertions must be intronic, and the "suppressed" phenotype is then caused by the T-DNA (Xue et al., 2012; Gao and Zhao, 2013; Sandhu et al., 2013; Osabe et al., 2017). In all cases a significant proportion of the large intron containing the T-DNA is correctly spliced, enhancing expression of the mutated gene and suppressing the phenotype. Although the mechanism is not well known, T-DNA hypermethylation and heterochromatinisation are necessary, and the RdDM (RNA-dependent DNA methylation) pathway is involved (Osabe et al., 2017). In our experiments, the altered phenotypes observed in the first generation of double homozygous mutant plants are "suppressed" by an increase of *MIT2* intron splicing.

3.3. Transcriptome of double homozygous mit1-1 mit2-1 mutant plants

No significant differences (except for *MIT* expression) were found between wild type plants and "compensated" *mit1-1mit2-1* double homozygous mutant plants, supporting the conclusion that partial expression (around 30 %) of MIT2 is sufficient for normal plant growth and development, at

least under standard growth conditions. In contrast, in the first generation of *mit1-1mit2-1* double homozygous mutant plants, which expressed 10-20 % of *MIT2* (at the transcript level), 408 genes are down-regulated (cluster 1) and 360 genes up-regulated (cluster 2) compared to wild type and compensated plants (Figure 9, Supplementary Tables S4 and S5).

Interestingly, data suggest down-regulation of the iron acquisition system. Besides *FRO2*, *IRT1* and *IRT2*, genes encoding either proteins involved in coumarin biosynthesis (F6'H1, feruloyl CoA ortho-hydroxylase 1; S8H, Scopoletin 8-hydroxylase; CYP82C4, fraxetin 5-hydroxylase) or coumarin export (ABCG37/PDR9) are included in cluster 1. These genes are part of the Fe deficiency response (Kobayashi and Nishizawa, 2012) and are regulated by the master transcription factor FIT1/FRU (Fe-deficiency induced transcription factor) which is also found in cluster 1 and known to control expression of additional cluster 1 genes involved in Fe homeostasis: *IREG2*, iron-regulated transporter 2/ferroportin 2; *BTSL2*, E3 ubiquitin ligase BRUTUS-like protein 2; and *MTPA2*, metal tolerance protein A2. Therefore, the response to a deficiency in iron uptake by mitochondria may be opposite to the response observed under Fe deficiency (reviewed in Kobayashi and Nishizawa, 2012; Riaz and Guerinot, 2021) and reminiscent of the root Fe exclusion strategy described in rice (Aung and Masuda, 2020).

Other enriched GO categories in cluster 1 related to root system may be indirectly relevant to iron acquisition (Supplementary Table S6): e.g. "root system development" (GO:0022622; FDR 5.2 x 10^{-34}, 3.7 fold enrichment), "root morphogenesis" (GO:0010015; FDR 6.1 x 10^{-23}, 5.9 fold enrichment), "root epidermal cell differentiation" (GO:0010053; FDR 4.3 x 10^{-11}, 8.8 fold enrichment) and "trichoblast differentiation" (GO:0010054; FDR 2.7 x 10^{-10}, 9.1 fold enrichment). Given the role of root epidermis and in particular of root hairs in water and nutrient uptake (Gilroy and Jones, 2000; Müller and Schmidt, 2004; Grierson et al., 2014), future work will be necessary to analyze root development in the mutant plants.

Relevant enriched GO terms in cluster 2 (up-regulated in mutant plants) may be involved in the observed pleiotropic phenotypes (Supplementary Table S7), for instance "plant organ formation" (GO:1905393; FDR 3.2 x 10^{-2}, 5.1 fold enrichment), "anatomical structure formation involved in morphogenesis" (GO:0048646; FDR 5.0 x 10^{-3}, 4.1 fold-enrichment), "flower development" (GO:0009908; FDR 4.4 x 10^{-4}, 3.5 fold enrichment) and "floral organ development" (GO:0048437; FDR 2.2 x 10^{-2}, 3.7 fold enrichment). Furthermore, the enriched GO categories "production of siRNA involved in gene silencing by small RNA" (GO:0070919; FDR 4.4 x 10^{-2}, 24.4 fold enrichment), which has three RNA-dependent RNA polymerases (RDR1, RDR2 and RDR3), and "heterochromatin assembly" (GO:0031507; FDR 2.3 x 10^{-2}, 7.9 fold enrichment), which contains the same three RDR, nucleolin 2 and two chromatin remodeling factors (chr31/SNF2 domain-containing protein CLASSY 3 and chr42/ SNF2 domain-containing protein CLASSY 2), may be relevant to explain the T-DNA suppression phenomenon discussed above.

Although enriched GO terms related to auxin were not found, careful examination of the genes in both clusters (Supplementary Tables S4 and S5) highlighted a number of genes related to either auxin metabolism, transport, signaling or response (9 in cluster 1, 13 in cluster 2). For instance, PIN2 (At5g57090), ABCG37/PDR9 (At3g53480), ABCB11 (At1g02520), ERULUS (At5g61350), MYB93 (At1g34670) and YUCCA3 (At1g04610) are down regulated in mutant plants (cluster 1). Other genes were found to be up-regulated (cluster 2), for example AIL7/PLT7 (At5g65510), LRP1 (At5g12330), SHI (At5g66350), SGR5 (At2g09140), SKP2A (At1g21410), ENP/MACCHI-BOU4/NPY1 (At4g31820), TCP18 (At3g18530) and GH3.5 (At4g27260). Whether these changes are related to the observed phenotypes similar to those of polar auxin transport mutants remains to be explored.

4. Materials and Methods

4.1. Plant material and growth conditions

All *A. thaliana* plants used were in the Columbia (Col-0) background. Seeds were sown on half-concentrated MS agar medium and stratified for 48 h at 4 °C in the dark. After two weeks in a 16 h/8

h day/night cycle at 22 °C, seedlings were transferred to soil and grown under long day conditions (16 h light/ 8 h dark).

Seeds from five T-DNA insertion mutants were obtained from the ABRC stock center: *mit1-1* (SALK_013388), *mit1-2* (SALK_208340C), *mit2-1* (SALK_096697), *mit2-2* (SAIL_653_B10, CS828300) and *mit2-3* (SALK_095187). For genotyping DNA was extracted from either 15 days-old seedlings or leaves of 4 weeks-old plants and analyzed as described (León et al. 2007). Primers used to amplify wild type and mutant alleles are described in Figure 1 and Supplementary Figures S2 and S3. To further characterize the T-DNA insertion in *mit2-1*, located in the intron spliced out in spite of its size, both T-DNA/*MIT2* junctions were amplified (Supplementary Figure S3). All amplified junctions were characterized by DNA sequencing.

Homozygous mutant *mit1-1* plants were crossed with either *mit2-1 or mit2-2* homozygous mutant plants. F1 seeds were germinated and F1 plants verified to be double heterozygous plants (genotype *MIT1mit1 MIT2mit2*). F2 seeds obtained from these selfed F1 plants were used to characterize F2 generation and obtain next generations (F3, F4 and so on).

4.2. Complementation of mutant Δmrs3Δmrs4 yeast cells

The *Δmrs3Δmrs4* strain (*MATa*, *ura3-52*, *leu2-3*, *112*, *trp1-1*, *his3-11*, *ade2-1*, *can1-100*(*oc*), *Δmrs3::kanMax Δmrs4::kanMax*) was kindly provided by Liangtao Li and Diane Ward (Department of Pathology, School of Medicine, University of Utah), and is described in Li and Kaplan (2004). The constructs containing the *ADH1* promoter, *MIT1* (At2g30160) or *MIT2* (At1g07030) cDNAs, and the *ADH2* terminator were generated using *in vivo* assembly yeast recombinational cloning (Oldenburg et al. 1997, Gibson et al. 2008). *ADH1* promoter and *ADH2* terminator were amplified by PCR using as template a plasmid kindly provided by Dr. Luis Larrondo, and Phusion High-Fidelity DNA polymerase (Thermo Scientific, https://www.thermofisher.com). For the promoter either primers 1 and 2 (with an overlap in its 5′ end with the beginning of *MIT2* cds) or primers 1 and 3 (with an overlap in its 5′ end with the beginning of *MIT1* cds) were employed, for the terminator either primers 8 (with an overlap in its 5′ end with the end of *MIT2* cds) and 9, or primers 10 (with an overlap in its 5′ end with the end of *MIT1* cds) and 9 were used. *MIT1* and *MIT2* cDNAs were obtained by RT-PCR. Total RNA was prepared from 15 day-old seedlings with the Spectrum Plant Total RNA kit (Sigma-Aldrich). cDNAs were synthesized with the Superscript First Strand synthesis system for RT-PCR (Invitrogen, Life Technologies), and PCR amplifications were performed with primers 4 and 5 for *MIT2*, and primers 6 and 7 for *MIT1*. PCR products were co-transformed with linear pRS426 plasmid into the BY4741 yeast strain (*MATa*, *his3Δ1*, *leu2Δ0*, *LYS2*, *met15Δ0*, *ura3Δ0*), and circular plasmids obtained from several ura+ colonies were transferred to E. coli DH5α. Positive colonies were identified by PCR, plasmids prepared (AxyPrep Plasmid Miniprep kit) and construct integrity verified by DNA sequencing. These plasmids were used to transform the *Δmrs3Δmrs4* strain and transformants were selected by plating on synthetic defined (SD) medium without uracyl. Complementation assays were performed growing yeast cells in liquid SD medium (without uracyl) to DO_{600nm} of 1.5, concentrating 5 times and plating serial dilutions onto agarose-SD plates with or without 50 μM of the impermeable iron chelator bathophenanthroline disulfonate (BPDS).

4.3. Expression analysis by RT-PCR and RT-qPCR

Total RNA was obtained from frozen seedlings with the TRIzol reagent, treated with DNase I (Promega, http://www.promega.com/) and quantified using a Nanodrop spectrophotometer (Thermo Scientific). cDNA synthesis was carried out on 1-2 μg of RNA, using oligodT as primer and SuperScript II Reverse transcriptase (Thermo Scientific).

To analyze *MIT* expression by RT-PCR in individual mutants, total RNA was prepared from 15 days-old seedlings. Then PCR reactions were performed with 1/10 of the cDNA and the following primer pairs (Supplementary Table S1): for *MIT1*, either primers 13 and 14 or 15 and 16; for *MIT2*, either primers 17 and 18 or 11 and 12.

For RT-qPCR total RNA was obtained from seedlings at stages 1.02 to 1.04 (Boyes et al., 2001). RT-qPCR experiments were performed on 1/10 of the cDNA using the StepOne Plus Real-Time PCR System (Applied Biosystems, http://www.appliedbiosystems.com/) according to the manufacturer's instructions and the Brilliant III Ultra-fast SYBR GREEN QPCR reagents (Agilent). RNA levels were estimated considering the amplification efficiency of each primer pair, and were normalized relative to either the clathrin adaptor (At4g24550) or the TIP41L (At4g34270) transcripts as internal controls. The primer pairs (Supplementary Table S1) used for clathrin adaptor were At4g24550F and At4g24550R, and for TIP41L At4g34270F and At4g34270R. Those for *MIT2* are indicated in figure legends. Primer sequences for *UPOX*, *MSM1*, *AOX1A*, *FRO2* and *IRT1* are also shown in Supplementary Table S1.

4.4. Transcriptome analysis by RNA sequencing

Total RNA was prepared from seedlings (stage 1.04) with the Spectrum Plant Total RNA Mini kit (Sigma-Aldrich). Following DNase I (Invitrogen, Life Technologies) treatment, RNA integrity was evaluated by capillary electrophoresis on a Qsep100 Bio-fragment analyzer (BiOptic, https://www.bioptic.com.tw). Libraries for RNA-Seq were prepared with the Illumina TruSeq Stranded mRNA kit, quantified by qPCR with KAPA Library Quantification Kit (Universal) (Roche, https://sequencing.roche.com), and sequenced using the NextSeq 500 System (Illumina, https://illumina.com), considering 150 bp paired-end reads. Raw sequences were processed with Trimmomatic v.0.39 (Bolger et al., 2014; http://www.usadellab.org), using the following settings: ILLUMINACLIP:TruSeq3-PE.fa:2:30:10:2:keepBothReads LEADING:30 TRAILING:30 SLIDINGWINDOW:10:30 MINLEN:36. Filtered sequences were mapped to the Arabidopsis genome (The Arabidopsis Information Resource TAIR v.10, www.arabidopsis.org) using HISAT2 v.2.1.0 with standard settings (Kim et al., 2019; http://daehwankimlab.github.io/hisat2/). Count tables were generated using the featureCounts function from the Rsubread (v.2.10.4) library from R (Liao et al., 2019), and the Araport11 GTF gene annotation (Cheng et al., 2017).

Differential gene expression between genotypes was analyzed with the DESeq2 package (v. 1.24) (Love et al., 2014), using the Likelihood ratio test (LRT). We considered differentially expressed genes those with $\log_2 > 1$ or $\log_2 < 1$, and adjusted p-value < 0.01. Clustering of differentially expressed genes was performed with the R library pheatmap v. 1.0.12 (kmeans_k = 2).

Overrepresentation of Gene Ontology (GO) terms (biological processes) was analyzed for each cluster using the PANTHER Overrepresentation Test tool (http://geneontology.org; Mi et al., 2013).

Supplementary Materials: The following supporting information can be downloaded at the website of this paper posted on Preprints.org, **Supplementary Figure S1.** *Arabidopsis MIT1 and MIT2 complement the growth defect of yeast ∆mrs3∆mrs4 in Fe-deficient medium.* Serial dilutions of the yeast ∆mrs3∆mrs4 strain transformed with a construct expressing either Arabidopsis MIT1 (AT2G30160) or MIT2 (AT1G07030) or with the pRS426 vector alone as a control were plated onto SD medium (solified with agarose to avoid Fe contamination and lacking uracyl) with or without the iron chelator BPDS.   **Supplementary Figure S2.** *Characterization of mutant mit1 alleles.* **(A)** Exon-intron structure of the *MIT1* gene with exons represented by boxes. Horizontal arrows indicate the position of primers and the T-DNA insertion sites are shown (T-DNA inserts are not drawn to scale). **(B)** Sequence of the *MIT1*/T-DNA junction in the *mit1-1* mutant allele. PCR amplification was performed using primers 13 and LBb1.3, and the product was sequenced. T-DNA is inserted 595 bp downstream of the ATG initiation codon, interrupting codon 200. In the alignment the first row corresponds to the left border T-DNA sequence (in blue), the third row to the wild type *MIT1* allele sequence (in red), and the second row to the junction between *MIT1* and T-DNA in the mutant allele (inserted nucleotides of unknown origin in green). **(C)** Sequence of the T-DNA/*MIT1*junction in the *mit1-2* allele. PCR amplification was performed using primers LBb1.3 and 14. T-DNA is inserted 154 bp downstream of the ATG initiation codon, interrupting codon 53. In the alignment the first row corresponds to the left border T-DNA sequence (in blue), the third row to the wild type *MIT1* sequence (in red), and the second row to the junction between T-DNA and *MIT1* in the mutant allele (inserted nucleotides of unknown origin in green). **Supplementary Figure S3.** *Characterization of mutant mit2 alleles.* **(A)** Exon-intron structure of the *MIT2* gene with exons represented by boxes. Horizontal arrows indicate the position of primers and the T-DNA insertion sites are shown (T-DNA inserts are not drawn to scale). **(B)** Sequences of the T-DNA/*MIT2* junctions in the *mit2-1* mutant allele. PCR amplifications were performed with

either primers LBb1.3 and 12 (3′ side of insertion) or primers 11 and RB (5′ side of insertion), and products were sequenced. T-DNA is inserted 419 bp downstream of the exon-intron junction, 18 nucleotides from the intron have been deleted (not shown) and 15 nucleotides of unknown origin inserted (in green). In the alignments first rows correspond to the left or right border T-DNA sequences (in blue), the third row to the wild type *MIT2* sequence (in red), and the second row to the junctions between *MIT2* and T-DNA in *mit2-1*. **(C)** Sequence of the *MIT2*/T-DNA junction in the *mit2-2* allele. PCR amplification was performed using primers 11 and LB1sail. T-DNA is inserted 712 bp downstream of the ATG initiation codon, interrupting codon 239. In the alignment the first row corresponds to the left border T-DNA sequence (in blue), the third row to the wild type *MIT2* sequence (in red), and the second row to the junction between *MIT2* and T-DNA in the mutant allele. **(D)** Sequence of the *MIT2*/T-DNA junction in the *mit2-3* allele. PCR amplification was performed using primers 11 and LBb1.3. T-DNA is inserted 500 bp downstream of exon-intron junction. In the alignment the first row corresponds to the left border T-DNA sequence (in blue), the third row to the wild type *MIT2* sequence (in red), and the second row to the junction between *MIT2* and T-DNA in the mutant allele. **Supplementary Figure S4.** *A significant proportion of seeds in plants with three mit mutated alleles have an abnormal phenotype.* Seed set per silique was scored along the main inflorescence axis for four F3 *MIT1mit1 mit2mit2* plants, four F3 *mit1mit1MIT2mit2* plants and two wild type plants. Silique 5 (older) to silique 16 (younger) were grouped in three groups of four siliques for each plant, and normal, abnormal and aborted seeds were counted in each of the 16 siliques of plants carrying three mutated alleles and the 8 siliques of Col-0 plants. Error bars are SD. **Supplementary Figure S5.** *Abnormal seeds from plants with only one wild type MIT allele germinate slowly.* Wild type seeds and both normal and abnormal seeds from *MIT1mit1-1 mit2-1mit2-1* plants were sown on 0.5 x MS, stratified for 48 h and grown for 3 and 4 days before being photographed. **Supplementary Figure S6.** *MIT2 expression in double homozygous mutant plants*. MIT2 expression levels were determined by RT-qPCR using primers 19 and 21 (Supplementary Table S1) and normalized to clathrin adaptor transcript level. Means ± SD of three biological replicates are shown. RNAs were prepared from 6-12 seedlings at stage 1.02 (Boyes et al., 2001), i.e. 12 days-old seedlings for wild type and 19 days-old seedlings for the first generation of the double homozygous mutant plants (*mit1-1mit1-1 mit2-1mit2-1*). Three asterisks indicate a value that was determined by the *t*-test to be significantly different from wild type (p < 0.001). To evaluate *MIT2* gene expression, primers 19 and 21 were used. **Supplementary Figure S7.** *Growth of double homozygous mutant plants was retarded throughout the entire life cycle*. Wild type Col-0 plants and double homozygous mutant plants (*mit1-1mit1-1 mit2-1mit2-1*, 1st generation) were grown as described in Materials and methods and three representative plants of each genotype were photographed at 2 months (**A**) and 3.5 months (**B**). **Supplementary Figure S8.** *Analysis of purified mitochondria from "compensated" double homozygous plants (mit1-1mit1-1 mit2-1mit2-1) and wild type plants.* (**A**) Proteomic analysis of the purified mitochondria (four mitochondrial preparations for each genotype). Heat map showing the relative abundance in both genotypes of 274 peptides corresponding to 108 polypeptides (Supplementary Table S3). Only the abundances of MIT1 (not detected in the mutant) and of MIT2 were significantly different (p < 0.001, *t-test*) between wild type and compensated plants. (**B**) Oxygen consumption by purified mitochondria using pyruvate, malate and ADP as substrates. Four mitochondrial preparations per genotype were tested and means ± SD are shown. Difference between genotypes is not significant (*t-test*). (**C**) BN-PAGE separation of respiratory chain complexes and supercomplexes followed by staining for Complex I activity (NADH:UQ oxidoreductase; right panel) and Coomassie blue staining (left panel). Three replicates (each 0.3 mg mitochondrial protein) of purified mitochondria from wild-type and "compensated" double homozygous seedlings were loaded. Mobility of respiratory complexes I, II, III, IV and V and supercomplexes are indicated.

Conflicts of Interest: The authors have no conflict of interest to declare

Abbreviations

BN-PAGE: blue native polyacrylamide gel electrophoresis; bp, base pair; BPDS, bathophenanthroline disulfonate; nt, nucleotide; GO, gene ontology; MIT, mitochondrial iron transporter; qRT-PCR: quantitative reverse transcription-PCR; RNA-seq, RNA sequencing.

References

1. Aida, M., Vernoux, X., Furutani, M., Traas, J. and Tsaka, M. (2002) Roles of PIN-FORMED1 and MONOPTEROS in pattern formation of the apical region of the Arabidopsis embryo. Development 129, 3965-3974.

2. Anders, S. and Huber, W. (2010) Differential expression analysis for sequence count data. Genome Biol. 11, R106. doi:10.1186/gb-2010-11-10-r106

3. Aung, M. S. and Masuda, H. (2020). How does rice defend against excess iron?: Physiological and molecular mechanisms. Front. Plant Sci. 11, 1102. https://doi.org/10.3389/fpls.2020.01102

4. Bashir, K., Ishimaru, Y., Shimo, H., Nagasaka, S., Fujimoto, M., Takanashi, H., Tsutsumi, N., An, G. and Nishizawa, N. K. (2011) The rice mitochondrial iron transporter is essential for plant growth. Nature Commun 2, 322.

5. Benjamins, R., Quint, A., Weijers, D., Hooykaas, P. and Offringa, R. (2001) The PINOID protein kinase regulates organ development in Arabidopsis by enhancing polar auxin transport. Development 128, 4057-4067.

6. Benková, E., Michniewicz, M., Sauer, M., Teichmann, T., Seifertová, D., Jürgens, G. and Friml, J. (2003) Local, efflux-dependent auxin gradients as a common module for plant organ formation. Cell 115, 591-602.

7. Bennett, S. R. M., Alvarez, J., Bossinger, G. and Smith, D.R. (1995) Morphogenesis in pinoid mutants of Arabidopsis thaliana. Plant J. 8, 505-520.

8. Bolger, A. M., Lohse, M. and Usadel, B. (2014) Trimmomatic: a flexible trimmer for Illumina sequence data. Bioinformatics 30, 2114-2120.

9. Boyes, D.C., Zayed, A.M., Ascenzi, R., McCaskill, A.J., Hoffman, N.E., Davis, K.R., et al. (2001) Growth stage-based phenotypic analysis of Arabidopsis: a model for hgh throughput functional genomics in plants. Plant Cell 13, 1499-1510.

10. Briat, J.F., Dubos, C., Gaymard, F. (2015) Iron nutrition, biomass production, and plant product quality. TRENDS in Plant Sci. 20: 33-40.

11. Chang, N., Sun, Q., Hu, J., An, C. and Gao, H. (2017) Large introns of 5 to 10 kilo base pairs can be spliced out in Arabidopsis. Genes 8, 200. doi: 10.3390/genes8080200

12. Cheng, C. Y., Krishnakumar, V., Chan, A. P., Thibaud-Nissen, F., Schobel, S. and Town, C. D. (2017) Araport11: a complete reannotation of the Arabidopsis thaliana reference genome. Plant J. 89, 789-804.

13. Christensen, S. K., Dagenais, N., Chory, J. and Weigel, D. (2000) Regulation of auxin response by the protein kinase PINOID. Cell 100, 469-478.

14. Clifton, R., Lister, R., Parker, K. L, Sappl, P. G., Elhafez, D., Millar, A. H., Day, D. A. and Whelan, J. (2005) Stress-induced co-expression of alternative respiratory chain components in Arabidopsis thaliana. Plant. Mol. Biol. 58, 193-212.

15. Collins J., Anderson G. (2012) Physiology of the Gastrointestinal Tract (Fifth Edition), Elsevier, New York.

16. Curie, C., Cassin, G., Couch, D., Divol, F., Higuchi, K., Le Jean, M., Misson, J., Schikora, A., Czernic, P., Mari, S. (2009). Metal movement within the plant: contribution of nicotianamine and yellow stripe 1-like transporters. Annals of botany, 103(1), 1–11.

17. De Longevialle, A. F., Meyer, E. H., Andrés, C., Taylor, N. L., Lurin, C., Millar, A. H. and Small, I. D. (2007) The pentatricopeptide repeat gene OTP43 is required for trans-splicing of the mitochondrial nad1 intron 1 in Arabidopsis thaliana. Plant Cell 19, 3256–3265. https://doi.org/10.1105/tpc.107.054841

18. Divol F, Couch D, Conéjéro G, Roschzttardtz H, Mari S, Curie C. (2013) The Arabidopsis YELLOW STRIPE LIKE4 and 6 transporters control iron release from the chloroplast. Plant Cell. 25(3):1040-55.

19. Duy, D., Wanner, G., Meda, A.R., Wiren, N. von, Soll, J. Philippar, K. (2007) PIC1, an Ancient Permease in Arabidopsis Chloroplasts, Mediates Iron Transport. Plant Cell, 19, 986–1006.

20. Eide, D., Broderius, M., Fett, J., Guerinot, M. L. (1996). A novel iron-regulated metal transporter from plants identified by functional expression in yeast. Proceedings of the National Academy of Sciences of the United States of America, 93(11), 5624–5628.

21. Eubel, H., Braun, H. P. and Millar, A. H. (2005) Blue-native PAGE in plants: a tool in analysis of protein-protein interactions. Plant Methods 1, 11. doi: 10.1186/1746-481I-I-II

22. Eubel, H., Jänsch, L. and Braun, H. P. (2003) New insights into the respiratory chain of plant mitochondria. Supercomplexes and a unique composition of complex II. Plant Physiol. 133, 274-286.

23. Foury, F. and Roganti, T. (2002) Deletion of the mitochondrial carrier genes MRS3 and MRS4 suppresses mitochondrial iron accumulation in a yeast frataxin-deficient strain. J. Biol. Chem. 277, 24475-24483.

24. Furutani, M., Vernoux, T., Traas, J., Kato, T., Tasaka, M. and Aida, M. (2004) PIN-FORMED1 and PINOID regulate boundary formation and cotyledon development in Arabidopsis embryogenesis. Development 131, 5021-5030.

25. Gao, Y. and Zhao, Y. (2013). Epigenetic suppression of T-DNA insertion mutants in arabidopsis. Mol. Plant 6, 539–545. https://doi.org/10.1093/mp/sss093

26. Guerinot M.L., Yi Y. (1994) Iron: nutritious, noxious, and not readily available. Plant Physiol. 104:815–820.

27. Gibson, D. G., Benders, G. A., Axelrod, K. C., Zaveri, J., Algire, M. A., Moodie, M., Montague, M. G., Craig Venter, J., Smith, H. O. and Hutchison III, C. A. (2008) One-step assembly in yeast of 25 overlapping DNA fragments to form a complete synthetic Mycoplasma genitalium genome. Proc. Nat. Acad. Sci. USA 105, 20404-20409.

28. Gilroy, S. and Jones, D. L. (2000) Through form to function: root hair development and nutrient uptake. Tr. Plant Sci. 5, 56-60.

29. Grierson, C., Nielsen, E., Ketelaarc, T. and Schiefelbein, J. (2014) Root Hairs. The Arabidopsis Book, 12, e0172. https://doi.org/10.1199/tab.0172

30. Haferkamp I, Schmitz-Esser S. (2012) The plant mitochondrial carrier family: functional and evolutionary aspects. Front Plant Sci. 8;3:2.

31. Ho, L. H., Giraud, E., Uggalla, V., Lister, R., Clifton, R., Glen, A., Thirkettle-Watts, D., Van Aken, O. and Whelan, J. (2008) Identification of regulatory pathways controlling gene expression of stress-responsive mitochondrial proteins in Arabidopsis. Plant Physiol. 147, 1858-1873.

32. Ivanova, A., Law, S. R., Narsai, R., Duncan, O., Lee, J-H., Zhang, B., Van Aken, O., Radomiljac, J. D., van der Merwe, M., Yi, K.   K. and Whelan, J. (2014) A functional relationship between auxin and mitochondrial retrograde signaling regulates Alternative Oxidase1a expression in Arabidopsis. Plant Physiol. 165, 1233-1254.

33. Jain, A., Dashner, Z. S. and Connolly, E. L. (2019) Mitochondrial iron transporters (MIT1 and MIT2) are essential for iron homeostasis and embryogenesis in Arabidopsis thaliana. Front. Plant Sci 10, 1449. doi: 10.3389/fpls.2019.01449

34. Jeong, J., Cohu, C., Kerkeb, L., Pilon, M., Connolly, E.L. Guerinot, M. Lou (2008) Chloroplast Fe(III) chelate reductase activity is essential for seedling viability under iron limiting conditions. Proc. Natl. Acad. Sci. U. S. A., 105, 10619–10624.

35. Kerchev, P. I., De Clercq, I., Denecker, J., Mühlenbock, P., Kumpf, R., Nguyen, L., Audenaert, D., Dejonghe, W. and Van Breusegem, F. (2014) Mitochondrial perturbation negatively affects auxin signaling. Mol. Plant 7, 1138-1150.

36. Kim, D., Paggi, J. M., Park, C., Bennett, C. and Salzberg, S. L. (2019) Graph-based genome alignment and genotyping with HISAT2 and HISAT-genotype. Nature Biotechnol. 37, 907-915.

37. Kim LJ, Tsuyuki KM, Hu F, Park EY, Zhang J, Iraheta JG, Chia JC, Huang R, Tucker AE, Clyne M, Castellano C, Kim A, Chung DD, DaVeiga CT, Parsons EM, Vatamaniuk OK, Jeong J. (2021) Ferroportin 3 is a dual-targeted mitochondrial/chloroplast iron exporter necessary for iron homeostasis in Arabidopsis. Plant J., 107:215-236.

38. Kobayashi, T. and Nishizawa, N. K. (2012) Iron uptake, translocation, and regulation in higher plants. Annu. Rev. Plant Biol. 63, 131–152.

39. Kolli, R., Soll, J. and Carrie, C. (2019) OXA2b is crucial for proper membrane insertion of COX2 during biogenesis of Complex IV in Plant Mitochondria. Plant Physiol. 179, 601–615.

40. Kühn, K., Obata, T., Feher, K., Bock, R., Fernie, A. R. and Meyer, E. H. (2015) Complete mitochondrial complex I deficiency induces an up-regulation of respiratory fluxes that is abolished by traces of functional complex I. Plant Physiol. 168, 1537-1549.

41. León, G., Holuigue, L. and Jordana, X. (2007) Mitochondrial complex II is essential for gametophyte development in Arabidopsis. Plant Physiol. 143, 1534-1546.

42. Li, L. and Kaplan, J. (2004) A mitochondrial-vacuolar signaling pathway in yeast that affects iron and copper metabolism. J. Biol. Chem. 279, 33653-33661.

43. Liao Y., Smyth G., Shi W. (2019) The R package Rsubread is easier, faster, cheaper and better for alignment and quantification of RNA sequencing reads, Nucleic Acids Research, 47:8.

44. Liu, C., Xu, A. and Chua, N. (1993) Auxin polar transport is essential for the establishment of bilateral simmetry during early plant embryogenesis. Plant Cell 5, 621-630.

45. Love, M.I., Huber, W. & Anders, S. (2014) Moderated estimation of fold change and dispersion for RNA-seq data with DESeq2. Genome Biol 15, 550.

46. Meyer, E. H., Tomaz, T., Carroll, A. J., Estavillo, G., Delannoy, E., Tanz, S. K., Small, I. D., Pogson, B. J. and Millar, A. H. (2009) Remodeled respiration in ndufs4 with low phosphorylation efficiency suppresses Arabidopsis germination and growth and alters control of metabolism at night. Plant Physiol. 151, 603-619.

47. Mi, H., Muruganujan, A., Casagrande, J. T. and Thomas, P. D. (2013) Large-scale gene function analysis with the panther classification system. Nature Prot. 8, 1551-1566. https://doi.org/10.2307/3869783

48. Mühlenhoff, U., Stadler, J. A., Richhardt, N., Seubert, A., Eickhorst, T., Schweyen, R. J., Lill, R. and Wiesenberger, G. (2003) A specific role of the yeast mitochondrial carriers Mrs3/4p in mitochondrial iron acquisition under iron-limiting conditions. J. Biol. Chem. 278, 40612-40620.

49. Müller, M. and Schmidt, W. (2004) Environmentally induced plasticity of root hair development in Arabidopsis. Plant Physiol. 134, 409-419.

50. Ohbayashi, I., Huang, S., Fukaki, H., Song, X., Sun, S., Morita, M. T., Tasaka, M., Millar, A. H. and Furutani, M. (2019) Mitochondrial pyruvate dehydrogenase contributes to auxin-regulated organ development. Plant Physiol. 180, 896-909.

51. Okada, K., Ueda, J., Komaki, M. K., Bell, C. J. and Shimura, Y. (1991) Requirement of the auxin polar transport system in early stages of Arabidopsis floral bud formation. Plant Cell 3, 677-684.

52. Oldenburg, K. R., Vo, K. T., Michaelis, S. and Paddon, C. (1997) Recombination-mediated PCR-directed plasmid construction in vivo in yeast. Nucleic Acids Res. 25, 451-452.

53. Osabe, K., Harukawa, Y., Miura, S. and Saze, H. (2017). Epigenetic Regulation of Intronic Transgenes in Arabidopsis. Sci. Rep. 7, 45166. https://doi.org/10.1038/srep45166

54. Papanikolaou G., Pantopoulos K. (2005) Iron metabolism and toxicity. Toxicol. Appl. Pharmacol. 202, 199–211.

55. Rajniak, J., Giehl, R. F. H., Chang, E., Murgia, I., von Wirén, N. and Sattely, E. S. (2018) Biosynthesis of redox-active metabolites in response to iron deficiency in plants. Nature Chem. Biol. 14, 442-450.

56. Restovic, F., Espinoza-Corral, R., Gómez, I., Vicente-Carbajosa, J. and Jordana, X. (2017) An active mitochondrial complex II present in mature seeds contains an embryo-specific iron–sulfur subunit regulated by ABA and bZIP53 and is involved in germination and seedling establishment. Front. Plant Sci. 8, 277. doi: 10.3389/fpls.2017.00277

57. Riaz, N. and Guerinot, M. L. (2021) All together now: regulation of the iron deficiency response. J. Exp. Bot. 72, 2045-2055.

58. Robinson, N. J., Procter, C. M., Connolly, E. L., Guerinot, M. L. (1999). A ferric-chelate reductase for iron uptake from soils. Nature, 397(6721), 694–697.

59. Roschzttardtz, H., Fuentes, I., Vásquez, M., Corvalán, C., León, G., Gómez, I., Araya, A., Holuigue, L., Vicente-Carbajosa, J. and Jordana, X. (2009). A nuclear gene encoding the iron-sulfur subunit of mitochondrial complex II is regulated by B3 domain transcription factors during seed development in Arabidopsis. Plant Physiol. 150, 84–95. doi: 10.1104/pp.109.136531

60. Sandhu, K. S., Koirala, P. S. and Neff, M. M. (2013) The ben1-1 brassinosteroid-catabolism mutation is unstable due to epigenetic modifications of the intronic T-DNA insertion. G3 (Bethesda) 3, 1587-1595.

61. Santi, S., Schmidt, W. (2009). Dissecting iron deficiency-induced proton extrusion in Arabidopsis roots. The New phytologist, 183(4), 1072–1084.

62. Schmidt SB, Eisenhut M, Schneider A. Chloroplast Transition Metal Regulation for Efficient Photosynthesis. Trends Plant Sci. 2020 Aug;25(8):817-828.

63. Tan YF, O'Toole N, Taylor NL, Millar AH (2010) Divalent metal ions in plant mitochondria and their role in interactions with proteins and oxidative stress-induced damage to respiratory function. Plant Physiol. 152, 747–761.

64. Tivendale ND, Belt K, Berkowitz O, Whelan J, Millar AH, Huang S. (2021) Knockdown of Succinate Dehydrogenase Assembly Factor 2 Induces Reactive Oxygen Species-Mediated Auxin Hypersensitivity Causing pH-dependent Root Elongation. Plant Cell Physiol. 62:1185-1198.

65. Tivendale ND, Millar AH. (2022) How is auxin linked with cellular energy pathways to promote growth? New Phytol. 2022 233:2397-2404.

66. Tsai, H. H., Rodríguez-Celma, J., Lan, P., Wu, Y. C., Vélez-Bermúdez, I. C. and Schmidt, W. (2018) Scopoletin 8-hydroxylase-mediated fraxetin production is crucial for iron mobilization. Plant Physiol. 177, 194-207.

67. Van Aken, O., Zhang, B., Carrie, C., Uggalla, V., Paynter, E., Giraud, E. and Whelan, J. (2009) Defining the mitochondrial stress response in Arabidopsis thaliana. Mol. Plant 2, 1310-1324.

68. Van Aken, O. and Whelan, J. (2012) Comparison of transcriptional changes to chloroplast and mitochondrial perturbations reveals common and specific responses in Arabidopsis. Front. Plant Sci. 3, 281. doi: 10.3389/fpls.2012.00281

69. Vert, G., Grotz, N., Dedaldechamp, F., Gaymard, F., Guerinot, M.L., Briat, J.F., Curie, C. (2002). IRT1, an Arabidopsis transporter essential for iron uptake from the soil and for plant growth. Plant Cell 14:1223-1233.

70. Vigani, G., Bashir, K., Ishimaru, Y., Lehmann, M., Casiraghi, F. M., Nakanishi, H., Seki, M., Geigenberger, P., Zocchi, G. and Nishizawa, N. K. (2016) Knocking down mitochondrial iron transporter (MIT) reprogramsprimary and secondary metabolism in rice plants. J. Exp. Bot. 67, 1357-1368.

71. Vigani G, Maffi D, Zocchi G. (2009) Iron availability affects the function of mitochondria in cucumber roots. New Phytol.,182:127-136.

72. Vigani G, Solti A, Thomine SB, Philippar K. (2019) Essential and Detrimental - an Update on Intracellular Iron Trafficking and Homeostasis. Plant Cell Physiol., 60:1420-1439.

73. Walter PB, Knutson MD, Paler-Martinez A, Lee S, Xu Y, Viteri FE, Ames BN. (2002) Iron deficiency and iron excess damage mitochondria and mitochondrial DNA in rats. Proc Natl Acad Sci U S A., 99:2264-9.

74.   Wang, Y., Lyu, W., Berkowitz, O., Radomiljac, J. D., Law, S. R., Murcha, M. W., Carrie, C., Teixera, P. F., Kmiec, B., Duncan, O., Van Aken, O., Narsai, R., Glaser, E., Huang, S., Roessner, U., Millar, A. H. and Whelan, J. (2016) Inactiavtion of complex I induces the expression of a twin cysteine protein that targets and affects cytosolic, chloroplastidic and mitochondrial function. Mol. Plant 9, 696-710.

75.   Xue, W., Ruprecht, C., Street, N., Hematy, K., Chang, C., Frommer, W. B., Persson, S. and Niittylä, T. (2012) Paramutation-like Interaction of T-DNA loci in Arabidopsis. PLoS ONE 7, e51651.

76.   Yi, Y., & Guerinot, M. L. (1996). Genetic evidence that induction of root Fe(III) chelate reductase activity is necessary foriron uptake under iron deficiency. The Plant journal: for cell and molecular biology, 10(5), 835–844.